T.C.
BAHCESEHIR UNIVERSITY
GRADUATE SCHOOL
DEPARTMENT OF BIOMEDICAL ENGINEERING

FOOTWEAR EFFECTS ON INSOLE–FORCEPLATE AGREEMENT VIA STATISTICAL PARAMETRIC MAPPING

MASTER'S THESIS

ASMA ALI MOHAMUD JAMA

ISTANBUL, 2025

T.C.
BAHCESEHIR UNIVERSITY
GRADUATE SCHOOL
DEPARTMENT OF BIOMEDICAL ENGINEERING

FOOTWEAR EFFECTS ON INSOLE–FORCEPLATE AGREEMENT VIA STATISTICAL PARAMETRIC MAPPING

MASTER'S THESIS

ASMA ALI MOHAMUD JAMA

THESIS ADVISOR

ASSIST. PROF. DR. BURCU TUNÇ ÇAMLIBEL

ISTANBUL 2025

T.C.
BAHCESEHIR UNIVERSITY
GRADUATE SCHOOL

11/04/2025

MASTER THESIS APPROVAL FORM

Program Name:	Biomedical Engineering Master Program
Student's Name and Surname:	Asma Ali Mohamud Jama
Name Of The Thesis:	Footwear Effects on Insole–Force Plate Agreement via Statistical Parametric Mapping
Thesis Defense Date:	11/04/2025

This thesis has been approved by the Graduate School which has fulfilled the necessary conditions as Master thesis.

Assoc. Prof. Yücel Batu SALMAN
Institute Director

This thesis was read by us, quality and content as a master's thesis has been seen and accepted as sufficient.

	Title, Name	**Institution**	**Signature**
Thesis Advisor	Asst. Prof. Burcu Tunç Çamlıbel	Bahçeşehir University	
2nd Member	Asst. Prof. Bora Büyüksaraç	Bahçeşehir University	
3th Member (Outside Institution)	Assist. Prof. Andaç Hamamcı	Yeditepe University	

I hereby declare that all information in this document has been obtained and presented in accordance with academic rules and ethical conduct. I also declare that, as required by these rules and conduct, I have fully cited and referenced all material and results that are not original to this work.

Name, Last Name: Asma Ali Mohamud Jama

Signature:

ABSTRACT

FOOTWEAR EFFECTS ON INSOLE–FORCEPLATE AGREEMENT VIA STATISTICAL PARAMETRIC MAPPING

Asma Ali Mohamud, JAMA
Master's Program in Biomedical Engineering
Supervisor: Assist. Prof. Dr. Burcu TUNÇ ÇAMLIBEL

April 2025, 61 Pages

This study investigates the agreement between insole pressure readings obtained from the Pedar system and force plate measurements during dynamic activities, under three distinct footwear conditions: flat shoes, running shoes with EVA gel midsoles, and Crocs. The primary objective was to evaluate the Pedar system's sensitivity, consistency, and overall reliability compared to the gold-standard force plate data. By exploring the compatibility of these two measurement systems, this research aims to contribute to the validation of wearable pressure-sensing technologies in real-world, dynamic settings.

Fifteen healthy adult participants performed walking and jumping tasks across all three footwear conditions. The vertical ground reaction force (Fz) and center of pressure (CoP) were extracted from both Pedar and force plate systems for comparative analysis. To comprehensively assess differences, a statistical parametric mapping (SPM) approach was employed, allowing for time-series statistical analysis across the gait and jump cycles.

The results revealed no statistically significant differences in CoP trajectories or vertical force profiles (Fz) among the three footwear conditions. This suggests that the Pedar system maintains a high level of consistency and reliability regardless of shoe type, even during high-impact and transitional movements such as jumping.

These findings hold important implications for biomechanics research and clinical gait analysis. They suggest that Pedar insoles can be confidently used as an

alternative to force plates in environments where portability, flexibility, and minimal setup are essential. Moreover, this study supports the integration of wearable insole technologies into routine movement assessments, rehabilitation monitoring, and ergonomic evaluations.

Keywords: Footwear, Pressure Measuring Insoles, Center of Pressure (CoP), Vertical Force (Fz), Statistical Parametric Mapping,

ÖZET

AYAKKABI TÜRLERININ PEDAR–KUVVET PLAKASI UYUMU ÜZERINDEKI ETKILERI: İSTATISTIKSEL PARAMETRIK HARITALAMA YÖNTEMIYLE DEĞERLENDIRME

Asma Ali Mohamud, JAMA

Biyomühendislik Yüksek Lisans Programı

Tez Danışmanı: Dr. Burcu TUNÇ ÇAMLIBEL

Nisan 2025, 61 sayfa

Bu çalışma, Pedar sisteminden elde edilen taban içi basınç ölçümleri ile kuvvet platformu verileri arasındaki uyumu, düz tabanlı ayakkabılar, EVA jel tabanlı koşu ayakkabıları ve Crocs olmak üzere üç farklı ayakkabı koşulunda dinamik aktiviteler sırasında incelemektedir. Birincil amaç, Pedar sisteminin hassasiyetini, tutarlılığını ve genel güvenilirliğini altın standart olan kuvvet platformu verileriyle karşılaştırarak değerlendirmektir. Bu iki ölçüm sistemi arasındaki uyumluluğun araştırılmasıyla, giyilebilir basınç algılama teknolojilerinin gerçek dünya dinamik koşullarında doğrulanmasına katkı sağlanması hedeflenmiştir.

On beş sağlıklı yetişkin katılımcı, üç ayakkabı koşulunun her birinde yürüme ve zıplama görevlerini gerçekleştirmiştir. Dikey yer tepkisi kuvveti (Fz) ve basınç merkezi (CoP), karşılaştırmalı analiz için hem Pedar hem de kuvvet platformu sistemlerinden elde edilmiştir. Farklılıkları kapsamlı bir şekilde değerlendirmek için, yürüme ve zıplama döngüleri boyunca zaman serisi istatistiksel analiz yapılmasına olanak tanıyan istatistiksel parametrik haritalama (SPM) yöntemi kullanılmıştır.

Sonuçlar, üç ayakkabı koşulu arasında CoP izlerinde veya dikey kuvvet profillerinde (Fz) istatistiksel olarak anlamlı bir fark bulunmadığını ortaya koymuştur. Bu durum, Pedar sisteminin, zıplama gibi yüksek darbe içeren geçişli hareketlerde dahi, ayakkabı tipinden bağımsız olarak yüksek düzeyde tutarlılık ve güvenilirlik sağladığını göstermektedir.

Bu bulgular, biyomekanik araştırmalar ve klinik yürüme analizleri açısından önemli sonuçlar taşımaktadır. Pedar tabanlıklarının, taşınabilirliğin, esnekliğin ve minimum kurulumun gerekli olduğu ortamlarda kuvvet platformlarına alternatif olarak güvenle kullanılabileceğini göstermektedir.

Anahtar Kelimeler: Ayakkabı, Basınç Ölçen Insole'lar, Basınç Merkezi, Dikey Kuvvet, İstatistiksel Parametrik Haritalama.

To women in STEM - breaking barriers and shaping the future.

ACKNOWLEDGEMENTS

First and foremost, I thank Allah for His endless grace and guidance. Without his blessings, none of this would have been possible.

I am deeply grateful to my supervisor, Dr. Burcu TUNÇ ÇAMLIBEL, for her unwavering support, wisdom, and dedication not only throughout my graduate studies but also during my undergraduate years. Her expertise and commitment have helped shape my academic journey.

To my parents, I owe everything. Their belief in me, even when I doubted myself, has been the foundation of my strength.

To my siblings, family, and friends, I am beyond thankful for their love and support.

I would also like to express my sincere gratitude to Elie Chebel, whose selfless support greatly contributed to this study, as well as to my colleagues and classmates for their invaluable collaboration.

TABLE OF CONTENTS

LIST OF TABLES

TABLES

LIST OF FIGURES

FIGURES

LIST OF ABBREVIATION

ANOVA	Analysis of Variance
AP	Anteroposterior
BW	Body Weight
CoP	Center of Pressure
EVA	Ethylene-Vinyl Acetate
FPFz	Force Plate Force
Fz	Vertical Force
GRF	Ground Reaction Force
IMU	Inertial Measurement Unit
ML	Mediolateral
PFT	Pedar Force Total
RMSD	Root Mean Square Difference
RMSE	Root Mean Square Error
SPM	Statistical Parametric Mapping

Chapter 1

Introduction

1.1 Background

The analysis of foot-ground kinetics, particularly through measuring the vertical ground reaction force (Fz) and the center of pressure (CoP), is fundamental in understanding human locomotion. Accurate characterization of these metrics enables clinicians and researchers to dissect movement patterns and interpret the resultant forces generated during dynamic activities such as walking, running, and jumping (Papagiannaki et al., 2020; Hollander et al., 2021). This biomechanical understanding holds significant importance across diverse fields, including clinical gait analysis, sports performance, injury prevention, and the design of functional footwear (Agresta et al., 2022; Menz & Bonanno, 2021). For instance, accurate kinetic data can facilitate the evaluation of recovery progress and inform sports training programs and equipment choices (Van Alsenoy et al., 2022; Sinclair et al., 2025). Thus, the reliability and precision of Fz and CoP measurements are essential, directly influencing the validity of research outcomes and the efficacy of resultant practical applications (Li et al., 2022).

In biomechanics, laboratory-based force plates are regarded as the 'gold standard' for precise measurement of ground response forces, including Fz, and for establishing the CoP trajectory due to their exceptional accuracy and reliability (Flores et al., 2018; Chander et al., 2021). These systems give important kinetic data, hence providing thorough analysis of the forces transferred during ground interaction (Li et al., 2022). Their main drawback, though, is their non portable nature and their constrained small area, which limits data gathering to controlled laboratory settings and makes them inappropriate for tracking ongoing movement or activities carried out in ecologically relevant environments such as outdoor terrain (Sinclair et al., 2021; Verheul et al., 2020).

Portable in-shoe pressure measuring solutions, such the Pedar insoles, have been created to get around this limitation. These systems directly measure plantar

pressure distribution inside the shoes, allowing for the following derivation or estimation of total Fz and CoP during different activities in more natural settings (Lippa et al., 2019; Horst et al., 2019). Though knowing the possible impact of shoes on these derived measurements is vital (Morrison et al., 2018). When evaluating Fz and CoP, one cannot ignore footwear since it is a vital interface in almost all instrumented biomechanical experiments conducted outside of barefoot settings. Studies have shown that the design and construction of shoes—including differences in cushioning, material stiffness, and general structure—significantly change plantar pressure distributions and affect lower limb kinematics and movement dynamics (Cho et al., 2022). Different kinds of footwear change the biomechanical loads the user experiences by altering the ground response forces and impact loading characteristics (Hébert-Losier et al., 2022; Gregory et al., 2018). Footwear's natural variability makes it more difficult to directly compare data gathered by in-shoe sensors, such the Pedar system which gauges pressure inside the shoe, and the ground truth kinetics measured by force plates under the shoe (Agresta et al., 2022). The particular shoes used thereby causes questions about the validity and dependability of Fz and CoP data produced by in-shoe pressure systems since the shoe itself alters the interaction being monitored (Jiang et al., 2021; Lindorfer et al., 2019).

While previous research has addressed the general validity of in-shoe pressure systems for estimating Fz and CoP relative to force plates, a significant gap persists concerning the specific influence of footwear on this measurement accuracy. Systematic investigations detailing how functionally distinct footwear types—ranging from minimal constructions like clogs to cushioned athletic shoes or standard flat shoes—impact the agreement between Pedar-derived kinetics and force plate measurements during dynamic activities such as walking, and jumping are notably lacking. Few studies have directly compared multiple, structurally different footwear conditions across a range of common dynamic tasks to quantify this interaction effect using detailed agreement metrics and temporal analysis methods. Therefore, the primary aim of the present study is to bridge this knowledge gap. By systematically comparing Fz and CoP measurements obtained simultaneously from the Pedar-X system and a laboratory force plate across three distinct footwear conditions (flat shoes, running shoes, and Crocs) during walking, single leg jumping, and vertical

jumping, this research seeks to quantify the influence of footwear type on the validity of in-shoe kinetic assessments during dynamic movement, utilizing metrics like Root-Mean-Square-Difference (RMSD), and waveform comparisons via Statistical Parametric Mapping (SPM).

1.2 Purpose of The Study

- To quantify the concurrent validity of the Pedar-X insole system by calculating the RMSD for Fz and CoP measurements along the mediolateral (ML) or X-axis, and anteroposterior (AP) or Y-axis, relative to a Bertec force plate, across three distinct footwear conditions (flat shoes, running shoes, Crocs) during walking, single leg jumping, and vertical jumping.
- To perform a detailed temporal comparison of Fz and CoP waveforms measured by the Pedar-X system and the force plate throughout the stance phase of walking, single leg jumping, and vertical jumps, utilizing 1D SPM to identify specific time intervals of significant divergence under each footwear condition.

1.3 Hypothesis

It was hypothesized that the type of footwear worn will significantly influence the overall agreement between the Pedar-X system and the force plate for both Fz and CoP measurements during dynamic activities. Specifically, we predict that flat shoes, providing a more direct interface, will yield the highest agreement (lowest RMSD, highest correlation), whereas cushioned running shoes, due to potential midsole compression and deformation, will exhibit the lowest agreement (highest RMSD, lowest correlation), with Crocs demonstrating intermediate or distinct patterns of agreement.

In addition, it is theorized that SPM analysis will reveal significant differences in the temporal accuracy of Fz and CoP waveforms between the Pedar-X and force plate contingent on footwear type. We predict that running shoes will result in larger magnitudes and/or longer durations of significant temporal divergence compared

to flat shoes, particularly during high-impact phases (e.g., landing, push-off) of single leg jumping and vertical jumping.

It is predicted that the agreement between Pedar-X and force plate measurements for both Fz and CoP will decrease (indicated by higher RMSD and potentially larger/longer SPM differences) as the dynamism of the task increases from walking to single leg jumping to vertical jumping, across all footwear conditions. It is further predicted that this task-dependent decrease in agreement will be most pronounced when participants are wearing running shoes.

Furthermore, it is hypothesized that CoP measurements derived from the Pedar-X system will exhibit greater sensitivity to footwear type (i.e., larger differences in RMSD and potentially more significant SPM divergence across footwear conditions) compared to the derived Fz measurements. This is proposed because CoP calculation relies on accurate spatial pressure distribution, which may be more susceptible to distortion by midsole compression or insole movement within different shoe structures than the total summed force (Fz).

1.4 Significance of the Study

- This research provides a quantitative characterization of the measurement error associated with the Pedar-X system for Fz and CoP assessment, when utilized with functionally distinct footwear types (flat shoes, running shoes, crocs). The measurements are taken during dynamic activities, thereby enhancing the critical interpretation of data obtained using in-shoe systems under varied conditions.

- The findings will yield evidence-based insights into the modulating effect of footwear on Pedar-X accuracy, offering practical guidance for methodological considerations and footwear selection criteria aimed at optimizing the validity of kinetic measurements derived from in-shoe pressure systems in both laboratory and field research.

- By systematically evaluating the agreement between Pedar-X and the force plate benchmark across common footwear and dynamic tasks, this study

contributes to a more informed assessment of the feasibility and inherent limitations of employing this portable technology for quantitative kinetic analysis in settings where force plates are unavailable.

- This study offers fundamental knowledge that can guide the future development of more precise measurement systems or maybe footwear-specific calibration or correction algorithms by advancing the knowledge of the intricate biomechanical interaction between dynamic loading conditions, sensor mechanics, and shoe structure.

1.5 Originality of the Study

The originality of this study mostly lies in its methodical analysis of how functionally different categories of common footwear alter the concurrent validity of Pedar-X derived kinetic measures (Fz and CoP) versus a force plate benchmark. Although earlier research validated in-shoe systems, they usually use one shoe type, compare shod with barefoot circumstances, or are missing a direct comparison across shoes with very varying structural and cushioning qualities.

This study specifically compares conventional flat shoes, cushioned running shoes, and minimally structured crocs, reflecting various construction paradigms pertinent to daily life and sports, and hence offering focused analysis of how particular shoe design ideas affect measurement accuracy. Moreover, evaluating this shoe impact throughout a range of dynamic activities—including walking, single leg jumping, and vertical jumping—helps to increase the uniqueness.

This multi-task strategy allows for an assessment of system agreement under different loading rates, magnitudes, and movement patterns typical of common functional and athletic activities, extending beyond many earlier validation experiments frequently restricted to walking. The study uses a thorough analytical framework combining standard discrete agreement metric with sophisticated temporal waveform analysis using SPM to provide a more thorough description of measurement differences across the whole movement cycle, coupled with this task variation.

The originality of this study comes from the integration of these components: the direct, systematic comparison of structurally diverse footwear types, the evaluation across several distinct dynamic tasks, and the application of detailed temporal analysis (SPM) alongside conventional discrete parameters statistics. Promising a uniquely nuanced knowledge of the footwear-sensor interaction, this multi-faceted approach directly addresses the noted gap in the literature on the quantified impact of shoe type on the accuracy of commonly used in-shoe systems for Fz and CoP measurement under dynamic conditions.

Chapter 2

Literature Review

2.1 Footwear and Its Biomechanical Impact

Beyond basic protection, footwear is essential in modifying lower limb function since it greatly affects plantar pressure distribution and gait mechanics, all of which are important in biomechanics, rehabilitation, and sports science. Different shoe styles originating from different philosophies—traditional, minimalist, and maximalist constructions—evoke various biomechanical reactions. For example, research indicates that while general shoe features have been proven to possibly affect gait negatively in both healthy people and clinical populations including Parkinson's disease (Reina-Bueno et al., 2021), minimalist shoes may help gait patterns deemed more natural than traditional shoes (Forczek et al., 2021). These results highlight the ability of shoe design to significantly change kinematic and kinetic factors during movement.

Shoe type and design characteristics have a major impact on variations in peak plantar pressure, a main measure of localized foot loading. Compared to typical shoes that tend to concentrate pressure in certain areas like the heel or forefoot, minimalist footwear usually encourages a more equal distribution of pressure across the plantar surface (Petersen et al., 2020). On the other hand, maximalist shoes can change normal foot mechanics and create distinct pressure profiles even with their dense cushioning; their particular design may even raise midfoot pressure (Gámez-Payá et al., 2021).

Footwear affects kinematic and kinetic components of gait as well. Certain kinds of shoes can change foot-strike patterns, stance time, and ground reaction force dynamics (Polomé et al., 2020). Heel-toe drop and sole flexibility are design features acknowledged as significant factors of lower limb kinematics; high-drop shoes may promote heel striking, while low-drop designs are usually linked with a forefoot strike pattern, therefore affecting load transmission through the lower limb (Zhang et al., 2021). This interaction generates continuous discussion about ideal shoe shape, usually stressing a trade-off between the apparent comfort of cushioning and the possible proprioceptive advantages provided by minimalist designs.

Particularly with regard to shock absorption, biomechanical study has concentrated mostly on footwear cushioning itself. Often examined are materials such ethylene vinyl acetate (EVA), as well as midsole shape and stack height influences. Although thicker midsoles could improve comfort and impact absorption, they could also change gait mechanics by changing sensory feedback from the foot (Moisan et al., 2020). This raises complicated questions like the "impact force paradox," which suggests that whereas very cushioned shoes could lower peak impact forces, they could also raise loading rates, a variable connected to the risk of musculoskeletal injury (Lieberman et al., 2010). Furthermore, the energy return properties of midsoles are a subject of debate, as potential improvements in running efficiency necessitate biomechanical modifications during gait (Hoogkamer et al., 2018).

Studies have also connected cushioning characteristics directly to plantar pressure distribution, with implications for therapeutic shoe design, such as illustrating that sufficient cushioning can significantly lower plantar pressure in diabetic patients, therefore helping ulcer prevention (Gámez-Payá et al., 2021). Moreover, the prolonged use of cushioned shoes can cause adaptive alterations in soft tissues and musculature, hence possibly causing overuse injuries (Miao et al., 2021). Methodological inconsistencies across studies and diversity in participant populations (Ramsey et al., 2023; Lin et al., 2022) have made it difficult, though, even with much study, to draw clear conclusions about ideal shoe traits, therefore stressing the need of ongoing research using varied samples and strong approaches.

2.2 Plantar Pressure Measurement Techniques

The measurement of plantar pressure distribution during gait is fundamental in biomechanics, as it provides thorough knowledge of foot function inaccessible by straightforward observation. In-shoe plantar pressure measuring devices are essential tools, usually utilising pressure sensors integrated into flexible insoles within footwear to collect data during normal walking.

A notable example is the Pedar system (Novel GmbH), which gathers real-time data on parameters including regional pressure, total force, contact area, and temporal aspects of foot contact using capacitive sensors (Salis et al., 2023; Das et al., 2024).

This feature provides clinicians and researchers strong capabilities to examine load distribution patterns and gait dynamics across many foot areas under ecologically feasible conditions.

The Pedar system's utility is well-documented in several disciplines. In shoe research, it helps to assess various shoe designs on pressure distribution, hence helping to maximize comfort and performance traits (Zwaferink et al., 2020). Clinically, in-shoe pressure analysis is essential for finding high-pressure locations linked with diabetic foot ulcer risk, therefore directing preventative efforts and the design of offloading approaches (Zwaferink et al., 2024; Castro-Martins et al., 2024). Within sports biomechanics, such systems help elucidate foot loading patterns during specific athletic tasks, contributing to performance optimization and injury prevention protocols (Soltani et al., 2021). Despite these advantages, limitations including sensor calibration drift, durability concerns, finite spatial resolution, and potential sensitivity to the in-shoe microclimate (temperature, humidity) have been reported (Zwaferink et al., 2024; Lambrich et al., 2023). Nonetheless, validation studies generally report acceptable reliability and validity for Pedar, suggesting its effectiveness for dynamic plantar pressure measurement despite these considerations (Lambrich et al., 2023).

Force plates represent a cornerstone technology in biomechanical analysis, widely regarded as the gold standard for accurately measuring ground reaction forces (GRFs) and the trajectory of the CoP during locomotion (HIROSE et al., 2025). Force plates offer exact, time-series kinetic data by means of piezoelectric or strain gauge sensors, hence measuring the foot's multidimensional ground forces (Lambrich et al., 2023). These are therefore crucial instruments for evaluating factors connected to gait stability, balance control, and the study of injury causes in both research and clinical environments. Their main drawback, then, is their fixed position, which usually limits analysis to a few steps inside a lab and prevents assessment while ambulation over different terrains (Zwaferink et al., 2024). Moreover, while great for measuring general forces and CoP, conventional force plates lack precise knowledge of the pressure distribution over the plantar surface itself (Salis et al., 2023).

Understanding the validity and complementing nature of these methods depends on direct comparisons between in-shoe systems like Pedar and force plates.

Researches with concurrent data gathering frequently find positive correlations for global parameters like total vertical force and CoP trajectories; measurements of peak force from Pedar show notable agreement with force plate data under controlled walking (Lambrich et al., 2023). This concordance implies that in-shoe devices can consistently record important features of the whole foot-ground contact usually evaluated with force plates.

Nonetheless, variations between the two methods have been gathered, especially with regard to changes in peak force magnitudes under particular circumstances and possible timing differences (Soltani et al., 2021). Differences in sensor properties, spatial resolution, and calibration techniques can help explain these discrepancies, occasionally causing changes in the detected sites of peak pressure (Zwaferink et al., 2024). These results underline the importance of methodical rigor and accurate calibration when applying in-shoe systems. Eventually, the continuous debate acknowledges the particular benefits of each technology: force plates provide a very consistent reference for global kinetic measurements; in-shoe systems shine at generating precise spatial and temporal pressure maps inside the shoe (Lambrich et al., 2023). Combining data from both technologies usually offers the most complete knowledge of foot biomechanics; ongoing developments in both systems hold the possibility of even better evaluation of foot dynamics in clinical, research, and performance settings.

2.3 Clinical and Occupational Relevance

Research on plantar pressure analysis and footwear biomechanics has notable practical consequences in several sectors, especially sports biomechanics, clinical gait evaluation, and occupational shoe design. Constant developments in measurement technology and a rising body of knowledge highlight the vital connections between shoe design features, human performance, health results, and safety. In sports biomechanics, understanding how plantar pressure, gait mechanics, and shoes interact shapes directly guides athletic shoe design. To maximize biomechanical stress during activities like running, some design elements such midsole characteristics, cushioning, stability, and flexibility can be modified, thereby improving performance and helping to prevent injuries (Malisoux et al., 2020; Agresta et al., 2022). Studies indicate that

custom-designed shoes fit to an athlete's biomechanics might enhance performance and energy economy (Honert et al., 2020).

Moreover, in sports science, plantar pressure monitoring is a useful technique for spotting unusual loading patterns usually linked with overuse injuries, such stress fractures (Knopp et al., 2023). Practitioners can understand injury risk factors by means of pressure profiles and offer athletes customized recommendations on shoe choice or training changes, hence supporting injury prevention efforts (Lambrich et al., 2023).

Studies linking modern shoe technology with swiftly racing times show how much performance may be enhanced by ideal shoe design (Knopp et al., 2023). Furthermore, biomechanical evaluations using pressure mapping help to clarify dynamic movements such as jumping and cutting, therefore allowing athletes and coaches to refine methods and increase efficiency by means of real-time feedback during training (Hoogkamer et al., 2018; Agresta et al., 2022; Zhang et al., 2021).

From the clinical point of view, the diagnosis, monitoring, and management of several disorders influencing gait and foot health have been fundamentally supported by plantar pressure analysis. It offers notable advantages for those with diseases including diabetic foot syndrome, foot deformities, and osteoarthritis (Castro-Martins et al., 2024), letting one see different pressure patterns as opposed to healthy people (Figure 1). In diabetic foot care, where recognizing areas of high pressure is essential for preventing ulceration, the capacity to map pressure distribution is very important (Malisoux et al., 2020). This information directs the prescription of custom orthotics meant to shift pressure away from sensitive areas and the application of shoe changes, hence reducing the risk of ulcers (Castro-Martins et al., 2024; Lambrich et al., 2023).

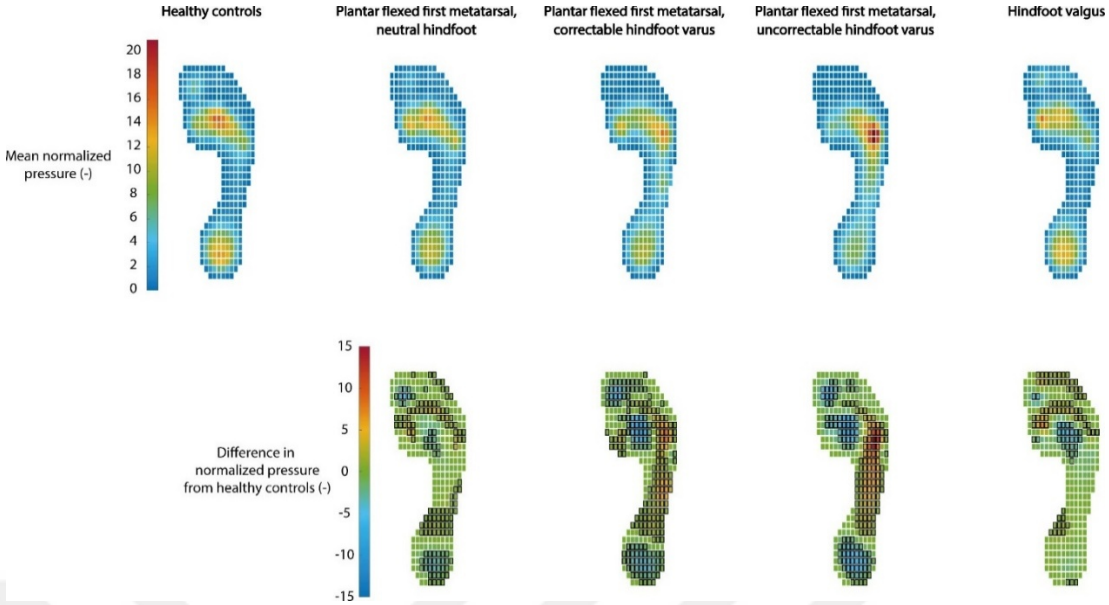

Figure 1. Mean normalized plantar pressure distributions in healthy controls and individuals with Hereditary Motor and Sensory Neuropathy (HMSN) classified by foot deformity type. Lower panels indicate significant differences ($p < 0.01$) from controls (red/yellow = increased pressure, blue = decreased pressure) (Bloks et al., 2023).

Plantar pressure monitoring has clinical use in preventive care and rehabilitation as well. It is used to objectively track the success of rehabilitation endeavors, evaluate gait symmetry, and measure patient recovery following surgery or stroke (Castro-Martins et al., 2024; Hoogkamer et al., 2018). Plantar pressure monitoring can also help fall risk assessment plans for susceptible populations, such elderly people (Menz & Bonanno, 2021; Lambrich et al., 2023). These analysis methods also greatly improve the design and assessment process for custom foot orthoses and prosthetics, therefore enabling more customization and better functional results for people with particular biomechanical requirements (Malisoux et al., 2020; Castro-Martins et al., 2024). Examining shoe biomechanics clearly helps to enhance patient results, hence supporting its clinical importance (Zhang et al., 2021).

Designing shoes that improve workers' safety and comfort in occupational environments depends on biomechanical concepts and plantar pressure data. Particularly for employees doing extended standing or manual handling duties, ergonomic factors seek to minimize weariness and lower the frequency of work-related musculoskeletal diseases (WMSDs) (Malisoux et al., 2020; Zhang et al., 2021).

Worker well-being is affected by features including cushioning, material stiffness, and general geometry, which affect plantar pressure distribution and comfort (Hoogkamer et al., 2018). Applying biomechanical knowledge to maximize both protection and functional design helps industries requiring certain shoes, such safety boots or anti-fatigue shoes, since different shoe types are linked with different injury risks in demanding work settings (Malisoux et al., 2020; Agresta et al., 2022). Data on plantar pressure can also guide more general ergonomic evaluations of jobs and workstations, thus ensuring greater alignment with human biomechanics to increase safety, lower the risk of injuries, and possibly boost production (Malisoux et al., 2020; Zhang et al., 2021; Menz & Bonanno, 2021). These uses taken together highlight the significant clinical and occupational value obtained from knowing and using plantar pressure dynamics and shoe biomechanics.

Chapter 3
Methodology

3.1 Participants

This study included fifteen healthy young adults—both male and female—between the ages of 18 and 30. The body weights of participants varied from 60 kg to 80 kg. Every participant was checked to make sure they had no history of lower limb injuries or musculoskeletal diseases in the last six months.

Furthermore, the experiment included only those with a clinically normal foot arch profile confirmed by a conventional arch height index evaluation.

Before data gathering, all subjects gave signed informed consent. Ethical clearance for the study came from the Research and Publication Ethics Board of Bahcesehir University. All experiments were conducted in the Bahcesehir University Biomedical Engineering Laboratory in Istanbul following the Helsinki Declaration's ethical guidelines.

3.2 Devices and Instrumentation

The BERTEC FP-4060-05-PT force platform (Bertec Corp.; Columbus, OH, USA) was utilized to measure the ground reaction forces in the study. This 600 mm x 400 mm platform records vertical force (Fz) and the CoP at a sampling frequency of 1000 Hz. The CoP is automatically calculated based on the vertical force component using the platform's six-component load transducers (Lambrich et al., 2023).

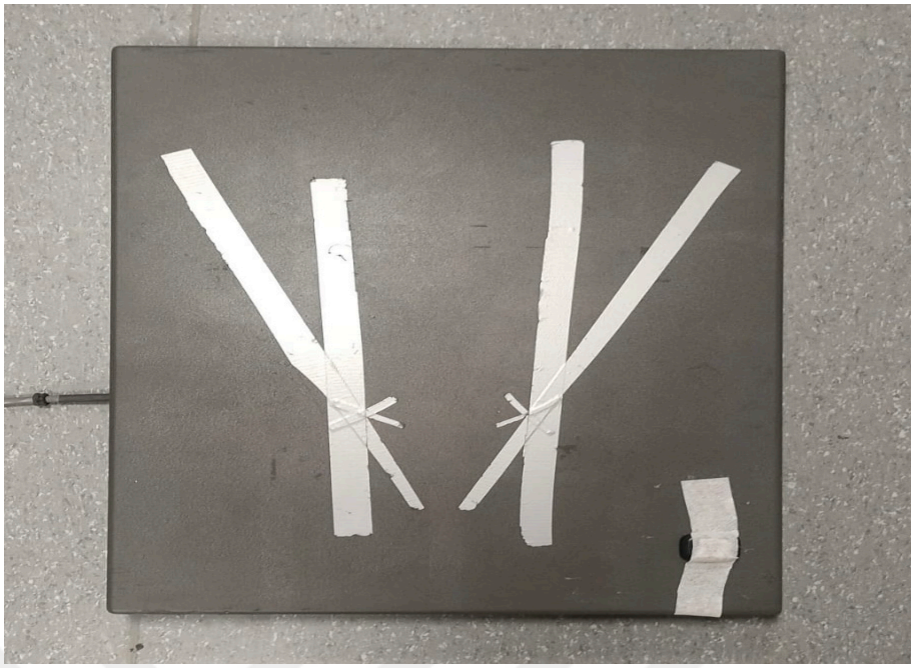

Figure 2. The BERTEC FP-4060-05-PT force plate used in the study.

The Pedar-X in-shoe pressure monitoring device (Novel GmbH, Munich, Germany) was used to record dynamic plantar pressure with great accuracy. Comprising a pair of flexible insoles, each integrated with 99 capacitive pressure sensors carefully spread throughout the plantar area, this advanced system is roughly 2.5 mm thick, and the entire insole thickness allows it to fit comfortably within conventional shoes without much change in natural foot mechanics.

Figure 3. Pedar-X pressure-measuring insoles used for capturing dynamic pressure data during various tasks to record the CoP and vertical forces.

Subject preparation and equipment setup were carried out carefully prior to the experiment's start to guarantee data accuracy, reduce signal artefacts, and preserve the lifetime of the system components. The instrumentation method guaranteed consistency throughout all data collecting sessions by means of a standardized process.

3.2.1 System initialization and hardware setup. Setting up the Pedar-X system started with establishing hardware connections. This dealt with checking the data collecting unit's correct power and operation, all system components' expected operation, and the active communication ports between the acquisition unit and the computer interface.

To avoid any unintentional cable disconnection during the experimental procedure, the cable routing was checked while subject was in standing and seated positions. The Pedar-X interface unit was then placed firmly around the subject's lower back or waist. This location guaranteed that the belt stayed unobtrusive and steady throughout the movement duration.

3.2.2 Insole placement and orientation. The insole connecting cables, attached to the straps on the Pedar-X belt, were then disconnected and prepared for connection. By placing the left insole cable on the left side of the body and the right cable on the right side, correct anatomical orientation was meticulously preserved. Maintaining consistent left-right mapping is critical during data collection. Every sensor-embedded insole was carefully put into the matching shoe. Poor placement could cause sensor damage or force and pressure measurement errors; thus, the insole has to remain level without bending, folding, or extreme compression.

3.2.3 Connecting and securing cables. Once the insoles were properly fitted within the shoes, their connectors were connected to the matching system belt sockets. To avoid any connection issues, labels marked "L" (left) and "R" (right) were matched properly. Reversed or mismatched cable connections could cause partial data acquisition, distorted pressure maps, or sensor reading gaps shown by the program.

To stabilize the cables during dynamic activities and reduce mechanical strain, straps were used to fasten each insole cable around the lower limbs starting at the ankle. Natural foot movements without cable tension were made possible by enough slack at the ankle. To lower cable movement or entanglement, extra straps were fastened around the calf and thigh. Meticulously coiling the extra wire length and fastening it to the belt ensured a neat and systematic arrangement.

3.2.4 Calibration procedure. The Pedar-X software interface was utilized to commence the calibration process once the subject was fully equipped and sitting in a relaxed posture. This meant carrying out a "zeroing" or "unloading" process whereby the subject stayed totally motionless with their feet unloaded. This important step guaranteed that the system logged only dynamic forces throughout the real trials and reset the baseline pressure values across all sensors. Correct calibration greatly improves the accuracy of the gathered pressure data and offers consistent comparisons across several sessions or shoe circumstances.

(A) (B)

Figure 4. Setup of the Pedar-X in-shoe pressure measurement system. The subject Pedar-X interface unit is secured around the lower back of the subject (A), insoles placed inside the shoes, and cables fastened using straps to ensure stable and accurate data collection (B).

3.2.5 Data acquisition. Plantar pressure data from the Pedar-X insoles were acquired at a sampling frequency of 100 Hz. The data was transmitted in real time to a computer via a previously established Bluetooth connection.

A Bertec force plate sampling at 1000 Hz was used for reference measurements to record GRFs and compute the related CoP trajectory.

Moreover, three Xsens DOT inertial measurement units (IMUs) were used to aid the Pedar system align with the force plate coordinate system: one sensor was attached to each foot and a third to the force plate surface. By means of this sensor

configuration, foot orientation could be estimated and any spatial difference between the two systems compensated, therefore enabling coherent coordinate transformations.

3.3 Experimental Protocol

In this study, participants were asked to wear three distinct types of footwear: flat shoes, cushioned running shoes with EVA-based midsoles, and Crocs. These shoe types were chosen to represent a variety of footwear designs with differing levels of cushioning, shock absorption, and structural support, allowing for a thorough comparison of how footwear affects foot pressure distribution and force measurements during dynamic tasks:

- Flat shoes, which feature minimalist soles without additional padding, were selected to serve as a baseline, providing insights into foot mechanics when minimal cushioning is provided.
- Cushioned running shoes with EVA gel midsoles were chosen for their superior shock absorption properties, which are intended to reduce the impact on joints during high-impact activities such as running and jumping.
- Finally, Crocs, made from lightweight foam material, offer moderate cushioning and flexibility, making them an interesting choice for evaluating how varying levels of foot protection and comfort affect pressure distribution.

Figure 5. Footwear types used in the study: flat shoes (minimalist soles), cushioned running shoes with EVA-based midsoles, and Crocs (lightweight foam material).

Each participant performed a series of five dynamic tasks, designed to assess foot pressure and force distribution during different types of movement. These tasks included both weight-bearing activities like walking and more dynamic, explosive movements like jumping, which challenge the foot's ability to absorb and redistribute forces:

- Task 1: Participants were instructed to walk at a normal pace, ensuring that their right foot made contact with the force plate for accurate measurements. This task served as a basic movement assessment, establishing a baseline for pressure measurements during walking.
- Task 2: The walking task was repeated, but this time the left foot was instructed to contact the force plate. This allowed for a comparison of pressure distribution between the dominant and non-dominant feet during similar walking conditions.

- Task 3: Participants performed a single-leg jump, landing on the force plate with their right leg. This task assessed the foot's ability to absorb impact during a dynamic, high-force activity using a single leg.
- Task 4: Following the same procedure as Task 3, participants performed a single-leg jump using their left leg. This allowed for an evaluation of how each foot, and footwear type, manages the forces associated with unilateral jumping.
- Task 5: Finally, participants performed a vertical jump, taking off and landing with both feet on the force plate. This task examined the combined impact forces generated during both a takeoff and landing in a bilateral jumping motion.

Each of the five tasks was performed while wearing all three footwear types, resulting in a total of 15 trials per participant (5 tasks × 3 footwear conditions). To ensure consistent data collection, participants were asked to perform eight steps (or movement cycles) for each task.

Footwear conditions were randomized across participants to minimize potential order effects and ensure that the results reflected the true influence of each shoe type on the biomechanical measurements. Additionally, participants were given ample time to acclimate to each footwear type before starting the trials to mitigate any discomfort or performance adjustments associated with wearing unfamiliar shoes.

This protocol allowed for a comprehensive comparison of foot pressure distribution and force measurement variability across different footwear types and dynamic tasks, providing a clearer understanding of how shoe design influences foot mechanics in both every day and high-impact movements.

3.4 Data Preprocessing

Signal processing was done using MATLAB (R2024b, The MathWorks Inc., Natick, MA, USA) following the collection of data. All done under a systematic and automated system to ensure consistency and reproducibility, this step included filtering, synchronization, and the calculation of error metrics.

3.4.1 Synchronization and resampling. To fit the Pedar-X sampling frequency, the force plate data, initially collected at 1000 Hz, were down-sampled to 100 Hz. The three heel taps at the start of each session served as alignment markers to temporally synchronize the datasets. These taps generated distinct peaks in the Fz signal, which were automatically detected using peak-finding algorithms. Corresponding accelerometer spikes from the Xsens DOT sensors were also identified to verify synchronization accuracy across all systems. By matching these events across the force plate, Pedar, and Xsens signals, the datasets were temporally aligned (Figure 9).

3.4.2 Normalization of vertical force (Fz). To account for inter-subject variability in body weight, the Fz values were normalized. Specifically, each Fz value was divided by the corresponding subject's body weight and then multiplied by 100. This procedure expresses the vertical force as a percentage of body weight.

$$\%\,\mathrm{BW}\,\mathrm{Fz} = \left(\frac{\mathrm{Fz\ (N)}}{\mathrm{Body\ Weight\ (N)}}\right) \times 100 \qquad (1)$$

3.4.3 Filtering and noise reduction. To reduce high-frequency noise, a fourth-order Butterworth low-pass filter was applied to all time-series data (CoP, Fz, and Acceleration) with a cutoff frequency of 10 Hz. This step was applied uniformly to all synchronized signals from Pedar, force plate, and Xsens systems.

3.4.4 Spatial alignment and orientation correction. Using the Xsens DOT sensors, the orientation of each foot during dynamic movements was computed and used to correct the spatial offset between the insole and the global reference frame defined by the force plate. The sensor fixed on the force plate was used as a stable anchor to determine the transformation matrix that brought the Pedar CoP into the same coordinate system as the force plate.

The data from the Xsens DOTs were processed to obtain rotation matrices that corrected for pitch, roll, and yaw in each trial. These matrices were then applied to the Pedar CoP signals to achieve spatial alignment. The process ensured that both CoP and vertical force data from the insole were directly comparable with those from the force plate across all movement directions.

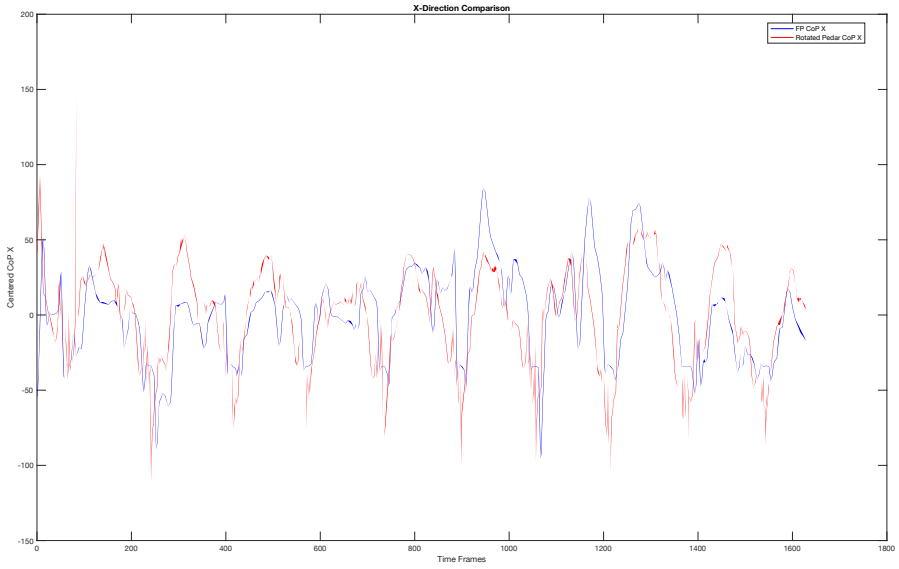

Figure 6. Rotated Pedar COPx, aligned using Xsens DOT orientation data, overlaid with force plate COPx for comparison.

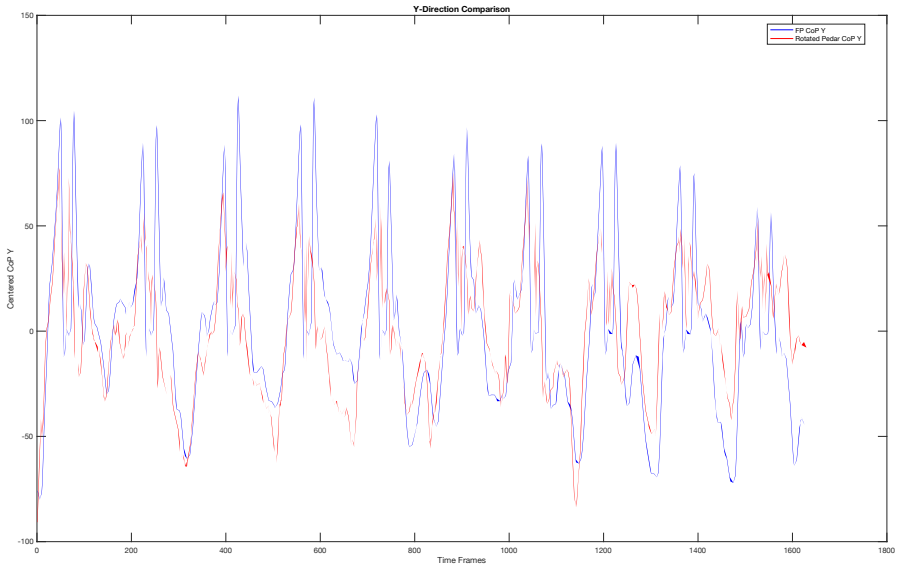

Figure 7. Rotated Pedar COPy, aligned using Xsens DOT orientation data, overlaid with force plate COPy for comparison.

3.4.5 Segmentation and step extraction. Each trial consisted of eight steps or movement cycles. Step segmentation was performed using peak detection in the vertical force (Fz) signal. The identified gait events (initial contact and toe-off) allowed the extraction of consistent 100-point time-normalized segments for each step or jump cycle. These normalized waveforms enabled direct comparison across steps, participants, footwear conditions, and systems.

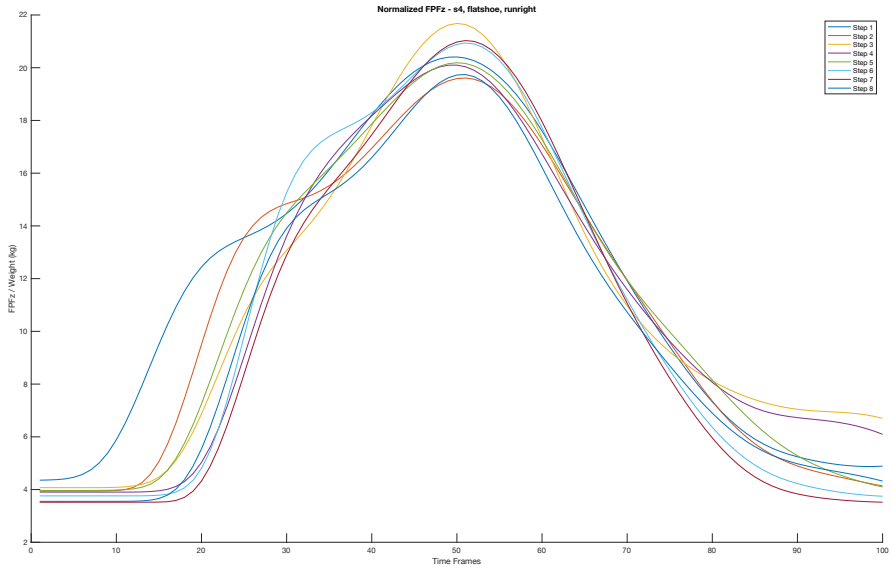

Figure 8. Normalized 8 jumping repetitions across all footwear in one subject.

A custom MATLAB script was developed to automate the extraction and processing of data from multiple `.mat` files, which were systematically organized for further analysis. The script looped through all the files and, for each trial, extracted the CoP and vertical force data, which were organized into structured tables for each step in the tasks. The following variables were computed or extracted for each step, and the underlying processes for their calculation are described in detail:

- FPCOPx and FPCOPy: These represent the force plate's CoP coordinates in the X and Y directions, respectively. The CoP provides a measure of the point of application of the resultant ground reaction force beneath the foot. To compute FPCOPx and FPCOPy, the force plate data (typically measured from multiple

force sensors) were used to calculate the weighted average of the force distribution across the plate's surface. The equation for the CoP is given by:

$$FPCOPx = \frac{\sum(Fi \cdot xi)}{\sum Fi}, \qquad FPCOPy = \frac{\sum(Fi \cdot yi)}{\sum Fi} \tag{2}$$

Where F_i is the force measured at sensor i, and x_i and y_i are the coordinates of sensor i. This computation provides the location of the CoP in both the ML and AP directions, respectively.

- InsoleX and InsoleY: These correspond to the CoP coordinates in the X and Y directions for the Pedar insole system. Similar to the force plate data, the Pedar insole measures pressure at multiple sensing points on the insole's surface. To compute InsoleX and InsoleY, the pressure distribution across the insole was weighted by the pressure values at each sensor, and the equations are analogous to those used for the force plate CoP:

$$InsoleX = \frac{\sum(Pi \cdot xi)}{\sum Pi}, \qquad InsoleY = \frac{\sum(Pi \cdot yi)}{\sum Pi} \tag{3}$$

Where P_i is the pressure measured at sensor i, and x_i and y_i are the coordinates of sensor i on the insole. This calculation provides the location of the CoP on the insole, reflecting how the force is distributed beneath the foot during dynamic activities.

- FPFz: This represents the vertical force measured by the force plate during each step. It is computed by summing the forces detected by each of the sensors on the force plate along the vertical axis. The total vertical force can be expressed as:

$$FPFz = \sum Fzi \tag{4}$$

Where F_{zi} is the vertical force component from sensor i on the force plate. This value provides an indication of the total vertical force exerted by the foot on the ground during a specific step.

- PFT: This variable represents the vertical force measured by the Pedar insole system. Similar to the force plate, the insole measures vertical pressure at each

sensing point. PFT is computed by summing the vertical pressure values across all sensors on the insole:

$$PFT = \sum P_{zi} \quad (5)$$

Where P_{zi} is the vertical pressure at sensor i on the insole. This calculation gives the total vertical force measured by the insole system during a specific step.

By organizing these variables into structured tables for each step of the dynamic tasks, the MATLAB script allowed for efficient comparison and analysis of the CoP and vertical force data from both the force plate and Pedar insole. These computations are essential for understanding the distribution of forces across the foot during dynamic tasks and for comparing the performance and accuracy of the insole-based measurement system against the gold standard of force plate data.

3.5 Statistical Analysis

To evaluate the agreement between the Pedar insole system and the force plate, RMSDx, RMSDy, and RMSDFz were calculated for each step. These metrics quantified the average magnitude of error in the ML and AP directions, as well as the Fz error which describes the vertical reaction force measurement.

$$RMSD = sqrt\left(\frac{1}{n} * \Sigma (x_i - y_i)^2\right) \quad (6)$$

Where:

- x_i = Data point from the force plate,
- y_i= Corresponding data point from the insole,
- n = Number of data points

Statistical analyses were performed at both discrete and waveform levels. The normality of data was first assessed using the Shapiro-Wilk test. Subsequently, for the normally distributed data a repeated-measures ANOVA was conducted, and if a significant difference was detected the Tukey post hoc test was used. While for the non-normally distributed data the non-parametric Friedman test was used, followed by

the Wilcoxon signed-rank test as a post hoc test. All statistical tests were carried out using SPSS (IBM® SPSS® Statistics 30, IBM Corp., USA). The significance level was at $p < 0.05$.

For waveform-level analysis, SPM-1D was employed to compare the full 100-point time-normalized signals of CoP and vertical force across devices. Paired t-test SPM{T} was conducted for each signal between both systems, offering a time-continuous view of measurement agreement and highlighting potential temporal differences between the Pedar and the force plate.

All data processing steps, including filtering, normalization, synchronization, RMSD calculation, and waveform comparison, were automated using custom MATLAB scripts to ensure efficiency and reproducibility. Ultimately, the preprocessed and segmented datasets were systematically arranged to allow group-level SPM analysis across all dynamic workloads and footwear conditions.

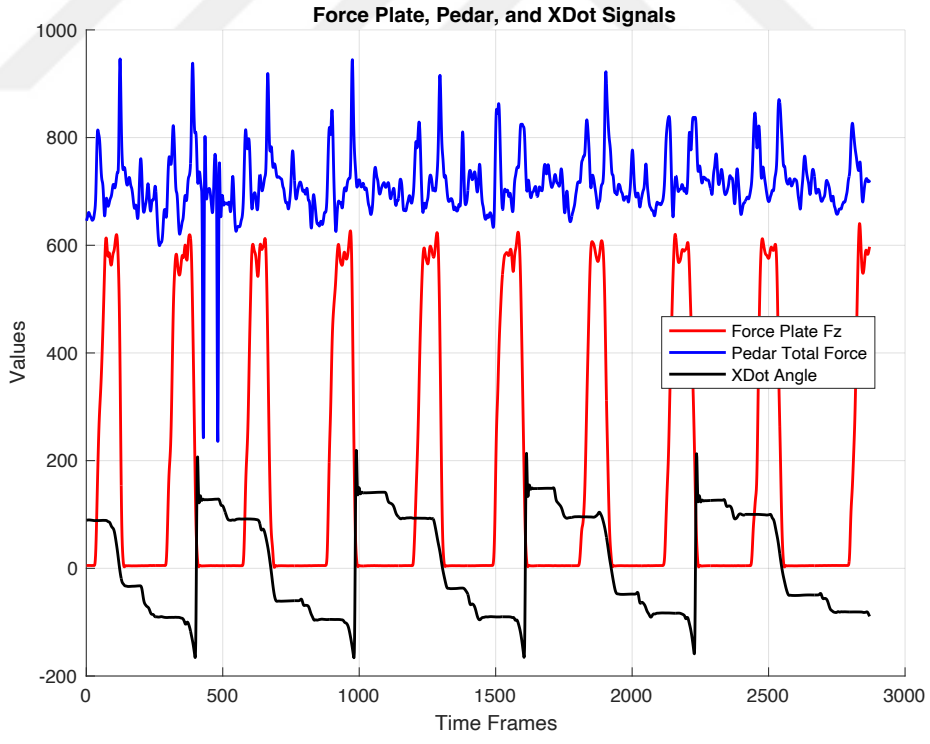

Figure 9. Synchronized Vertical Force of Pedar-X, Force plate and Acceleration from Xsens Dot.

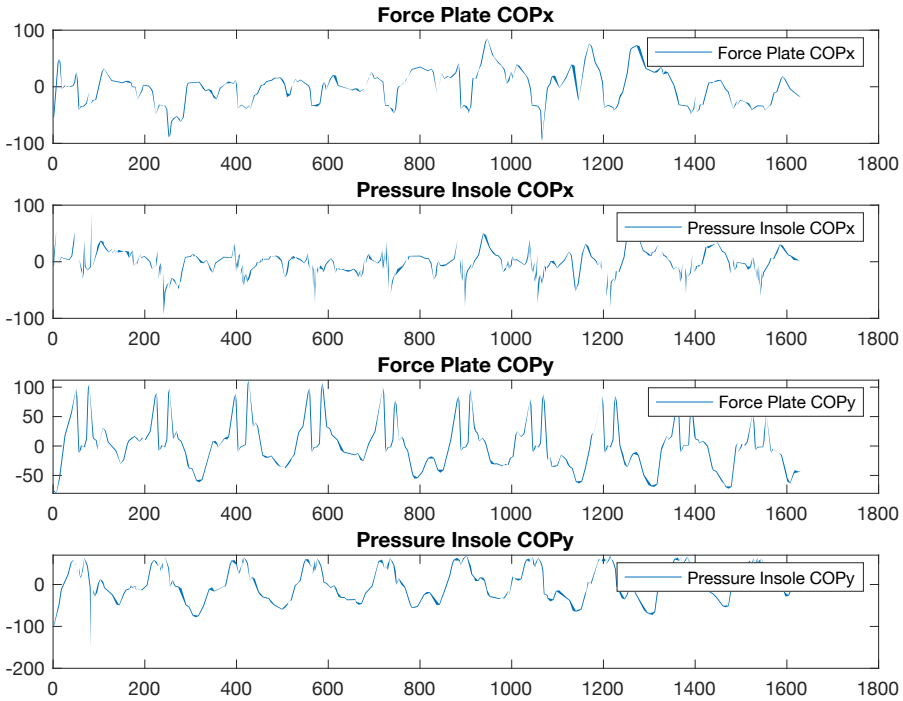

Figure 10. COPx, COPy readings from Forceplate against Pedar Insoles.

Chapter 4

Results

4.1 General Findings

To assess the influence of distinct types of footwear on foot pressure measurements recorded by pressure insoles, the RMSD and standard deviation (SD) were calculated across different footwear conditions across all tasks for three dimensions: ML (X-axis), AP (Y-axis), and vertical force (Fz). The RMSD values were then combined and the mean and standard deviation for each footwear condition were calculated. The resultant means and standard deviations are summarized in Table 1.

Along the ML axis, the RMSDx results showed slightly smaller errors compared to the AP axis. The highest mean RMSD was recorded for "Crocs" (75.02 ± 18.31 mm), followed by "Runningshoe" (72.65 ± 12.88 mm) and "Flatshoe" (68.58 ± 7.36 mm). Nevertheless, no statistically significant differences among footwear types in ML pressure estimations was revealed ($p = 0.247$).

Along the AP axis (RMSDy), all footwear types presented comparable error levels. The descriptive statistics indicated that the highest mean RMSD was observed in the "Crocs" condition (89.14 ± 27.34 mm), followed by the "Runningshoe" (85.96 ± 19.52 mm) and "Flatshoe" (81.44 ± 21.48 mm) conditions. The computed p-value showed no significant difference ($p = 0.766$).

As for the vertical ground reaction force estimations (RMSDFz), the descriptive statistics demonstrated that the "Crocs" condition exhibited the highest mean RMSD (68.85 ± 38.10 %BW), followed by the "Runningshoe" (63.53 ± 27.23 %BW) and "Flatshoe" (54.26 ± 24.68 %BW) conditions. Again, no statistically significant effect of footwear was revealed ($p = 0.175$).

Table 1

Mean ± SD of RMSD Measurements Across Footwear Types

Footwear	RMSDy (mm)	RMSDx (mm)	RMSDFz (%BW)
Crocs	89.14 ± 27.34	75.02 ± 18.31	68.85 ± 38.10
Flatshoe	81.44 ± 21.48	68.58 ± 7.36	54.26 ± 24.68
Runningshoe	85.96 ± 19.52	72.65 ± 12.88	63.53 ± 27.23

4.2 Crocs

4.2.1 Jump task. As shown in Table 2, the RMSDx values for crocs during this task across all subjects fell within a range of 18.19 mm and 90.97 mm with a mean of 44.61 ± 21.91 mm ($p = 0.162$). Along the Y-axis, the mean RMSDy value for Crocs was 44.55 ± 12.99 mm with values ranging from 34.23 mm to 71.23 mm ($p = 0.819$). Along the Z-axis the mean RMSDFz value for Crocs was found to be 50.47 ± 51.73 %BW with values ranging between 14.69 %BW and 207.92 %BW ($p = 0.695$).

The SPM analysis for the Crocs condition during the jump task showed 2 significant difference points (~52-54%) in the COPx between the Pedar insole and the force plate. In parallel, only 2 significant difference points were observed with respect to COPy between the Pedar insole and the force plate (~38-40%). Conversely, no significant differences were found in the Fz between the Pedar insole and the force plate (Figure 11).

Table 2

Crocs footwear RMSDx, RMSDy, and RMSDFz values across Jump task

Subject ID	RMSDx (mm)	RMSDy (mm)	RMSDFz (%BW)
1	57.44	34.23	65.44
2	74.29	68.84	207.92
3	28.98	36.92	17.73
4	20.25	37.75	16.54
5	65.37	42.27	14.69
6	18.19	38.83	22.33
7	37.41	35.85	41.10
8	32.04	38.91	27.45
9	90.97	64.50	100.07
10	24.22	39.45	36.78
11	57.47	71.23	76.16
12	26.35	36.65	14.88
13	62.33	51.86	79.82

Table 3 (cont'd)

Subject ID	RMSDx (mm)	RMSDy (mm)	RMSDFz (%BW)
14	36.41	35.72	20.02
15	37.50	35.24	16.12
Mean	44.61	44.55	50.47
(SD)	(± 21.91)	(± 12.99)	(± 51.73)

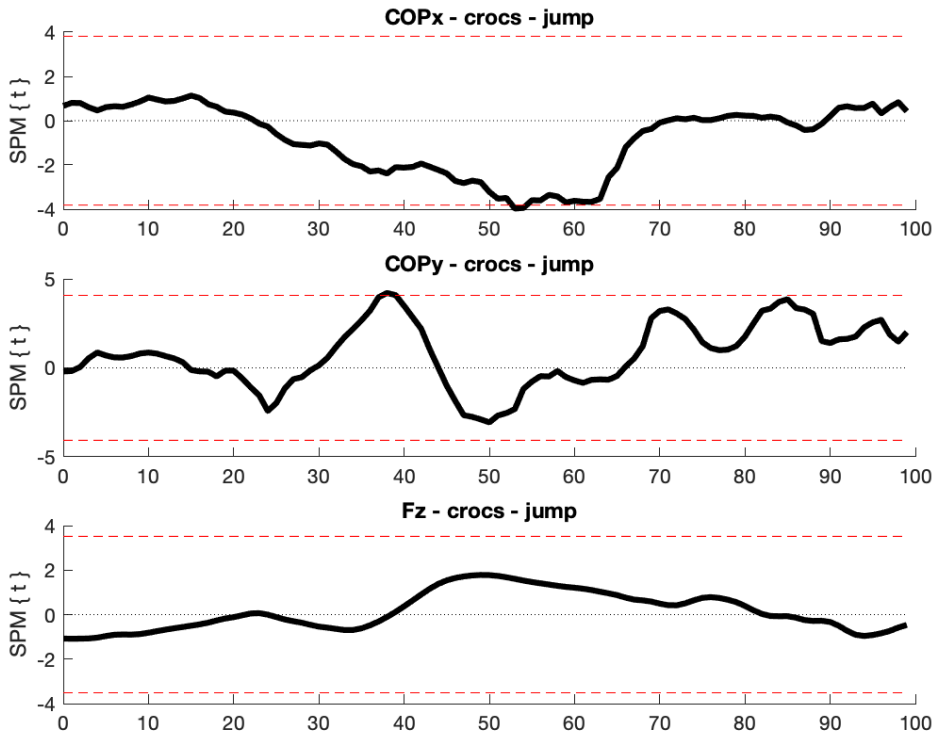

Figure 11. Statistical Parametric Mapping of COPx, COPy, and Fz in Crocs footwear during Jumping task.

4.2.2 Single leg jump left task. As presented in Table 3, a high mean RMSDx was demonstrated by crocs (87.07 ± 29.10 mm), with values ranging between 44.49 mm and 162.18 mm (p = 0.043). For the y-axis, an average RMSDy of (116.80 ± 54.81 mm) was observed with values ranging between 52.01 mm and 237.41 mm (p = 0.017). The average RMSDFz value for Crocs in this task was 97.79 ± 68.91 (p = 0.206) with values ranging between 20.11 %BW and 271.80 %BW across all subjects.

In the Single Leg Jump left task, Crocs displayed 29 points of deviation around (~20-30%), (~39-49%), and (~61-70%) in the COPx. No significant difference was

observed in the COPy. Conversely, Crocs exhibited a large significant difference around (~22-75%) of the cycle along the Fz (Figure 12).

Table 4

Crocs footwear RMSDx, RMSDy, and RMSDFz values across Single Leg Jump left task

Subject ID	RMSDx (mm)	RMSDy (mm)	RMSDFz (%BW)
1	94.88	237.41	191.58
2	62.01	146.97	271.80
3	66.36	102.12	20.11
4	44.49	88.64	38.60
5	86.37	142.61	61.44
6	90.52	49.57	52.01
7	58.87	92.10	49.12
8	118.67	52.01	110.42
9	112.47	189.07	178.89
10	67.84	118.27	57.48
11	88.14	170.47	95.91
12	96.26	53.68	88.18
13	89.14	131.42	63.85
14	162.18	59.45	128.58
15	67.84	118.27	58.81
Mean (SD)	87.07 (± 29.10)	116.80 (± 54.81)	97.79 (± 68.91)

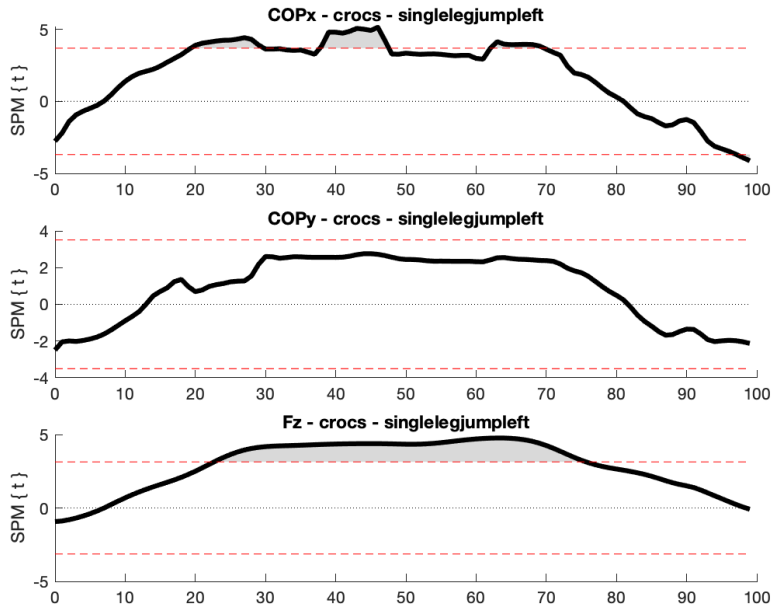

Figure 12. Statistical Parametric Mapping of COPx, COPy, and Fz in Crocs footwear during Single Leg Jump left task.

4.2.3 Single leg jump right task. Crocs presented a high mean RMSDx value (95.68 ± 36.52 mm) while the RMSD values fell between 46.76 mm and173.25 mm ($p = 0.758$). As for the RMSDy, the RMSD calculated ranged between 31.67 and 201.78 ($p = 0.247$) with a mean value of 114.97 ± 48.48 mm was exhibited by the crocs. Along the vertical axis, The mean RMSD was 77.32 ± 48.79 %BW ($p = 0.743$) while values spanned between 34.51 %BW – 166.79 %BW. (Table 4) across all subjects.

In the Single Leg Jump right task, Crocs displayed a significant deviation around (~47-73%) of the cycle in COPx. Complementary results were observed in COPy where Crocs exhibited significant difference in 20 significant points of the cycle (~55-75%). For Fz, Crocs demonstrated significant difference in the middle stages of the cycle (~30-74%) (Figure 13).

Table 5

Crocs footwear RMSDx, RMSDy, and RMSDFz values across Single Leg Jump right task

Subject ID	RMSDx (mm)	RMSDy (mm)	RMSDFz (%BW)
1	111.44	201.78	151.99
2	93.21	147.66	166.79

Table 4 (cont'd)

Subject ID	RMSDx (mm)	RMSDy (mm)	RMSDFz (%BW)
3	57.59	124.79	28.72
4	61.04	101.12	24.09
5	65.07	113.37	22.70
6	46.76	105.85	117.99
7	89.33	48.52	42.10
8	75.85	126.44	36.47
9	147.03	31.67	136.48
10	149.99	192.07	74.89
11	84.45	126.81	34.51
12	98.63	137.50	91.52
13	101.26	43.14	65.32
14	80.37	130.29	58.13
15	173.25	93.54	108.08
Mean (SD)	95.68 (± 36.52)	114.97 (± 48.48)	77.32 (± 48.79)

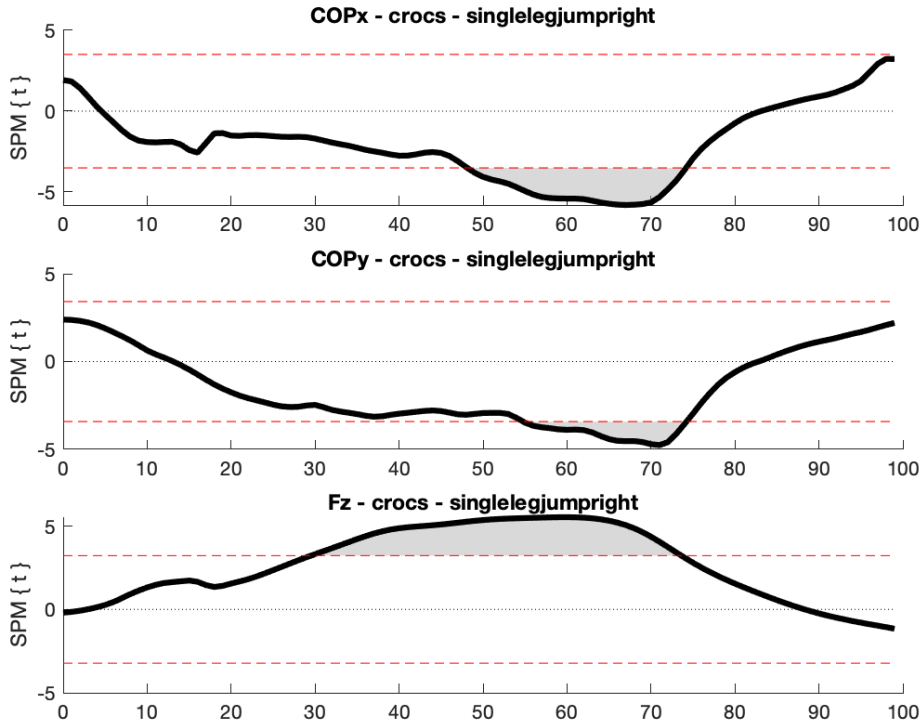

Figure 13. Statistical Parametric Mapping of COPx, COPy, and Fz in Crocs footwear during Single Leg Jump right task.

4.2.4 Walk left task. The RMSD along the x-axis in the crocs condition showed a mean of (77.08 ± 18.96 mm) with values between 46.26 mm to 107.34 mm ($p = 0.084$). Moving along the y-axis, the. RMSDy values ranged between 29.00 mm and 163.2 mm with a mean of 84.86 ± 39.51 mm ($p = 0.127$). The vertical force RMSD values ranged between between 27.09 %BW and 122.69 %BW resulting in a mean of 57.20 ± 28.98 %BW ($p = 0.221$) among all subjects (Table 5).

In the Walk left task, Crocs displayed a large significant deviation around (~20-64%) of the cycle in COPx. In COPy, Crocs exhibited minimal significant difference (~32-36%) and (~60-64%). As for Fz, large significant differences were noted in most parts of the cycle (~20-72%) (Figure 14).

Table 6

Crocs footwear RMSDx, RMSDy, and RMSDFz values across Walk left task

Subject ID	RMSDx (mm)	RMSDy (mm)	RMSDFz (%BW)
1	85.38	163.23	122.69
2	50.84	102.78	88.95
3	66.69	106.79	33.99
4	46.26	73.97	42.68
5	52.87	83.84	31.22
6	82.02	105.74	65.29
7	96.83	32.28	54.94
8	81.16	103.89	103.71
9	100.50	31.38	63.04
10	87.59	111.55	32.41
11	63.16	114.72	29.86
12	67.85	109.06	70.08
13	95.10	30.65	39.42
14	72.61	74.05	52.62
15	107.34	29.00	27.09
Mean (SD)	77.08 (± 18.96)	84.86 (± 39.51)	57.20 (± 28.98)

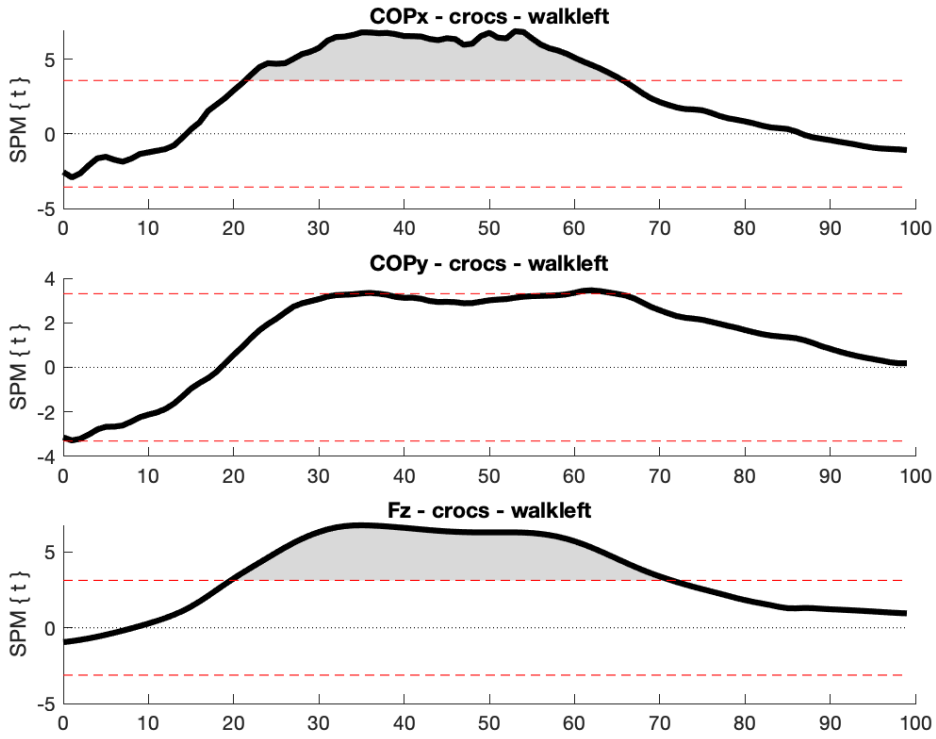

Figure 14. Statistical Parametric Mapping of COPx, COPy, and Fz in Crocs footwear during Walk left task.

4.2.5 Walk right task. As illustrated in table 6, for all subjects, the RMSD values along the X-axis fell within the range of 43.81-115.18 yielding to a high RMSDx mean (70.72 ± 28.53 mm; p = 0.302). Across the Y-axis, the crocs exhibited a mean RMSDy of 84.49 ± 37.11 mm with values ranging between 32.56 mm and 143.54 mm (p = 0.766). Along the vertical plane (Z-axis), the RMSDFz values varied between 21.16 %BW to 203.70 %BW with a mean 61.46 ± 45.02 %BW (p = 0.280).

In the Walk right task, Crocs displayed a large significant deviation around (~19-59%) of the cycle in COPx. In COPy, Crocs exhibited significant difference in midstance of the cycle (~40-54%). For Fz, Crocs exhibited 48 significant difference points in the cycle (~24-72%) (Figure 15).

Table 7

Crocs footwear RMSDx, RMSDy, and RMSDFz values across Walk right task

Subject ID	RMSDx (mm)	RMSDy (mm)	RMSDFz (%BW)
1	87.10	143.54	89.33
2	59.71	115.93	85.92

Table 6 (cont'd)

Subject ID	RMSDx (mm)	RMSDy (mm)	RMSDFz (%BW)
3	50.90	112.19	50.22
4	43.81	83.21	38.20
5	57.51	85.19	31.28
6	20.82	75.87	203.70
7	105.30	33.15	44.96
8	89.34	146.35	86.68
9	115.18	38.87	56.53
10	46.61	68.61	29.23
11	63.09	102.25	21.16
12	50.63	94.70	60.92
13	97.52	32.56	41.67
14	59.78	94.59	54.53
15	113.43	40.36	27.54
Mean (SD)	70.72 (± 28.53)	84.49 (± 37.11)	61.46 (± 45.02)

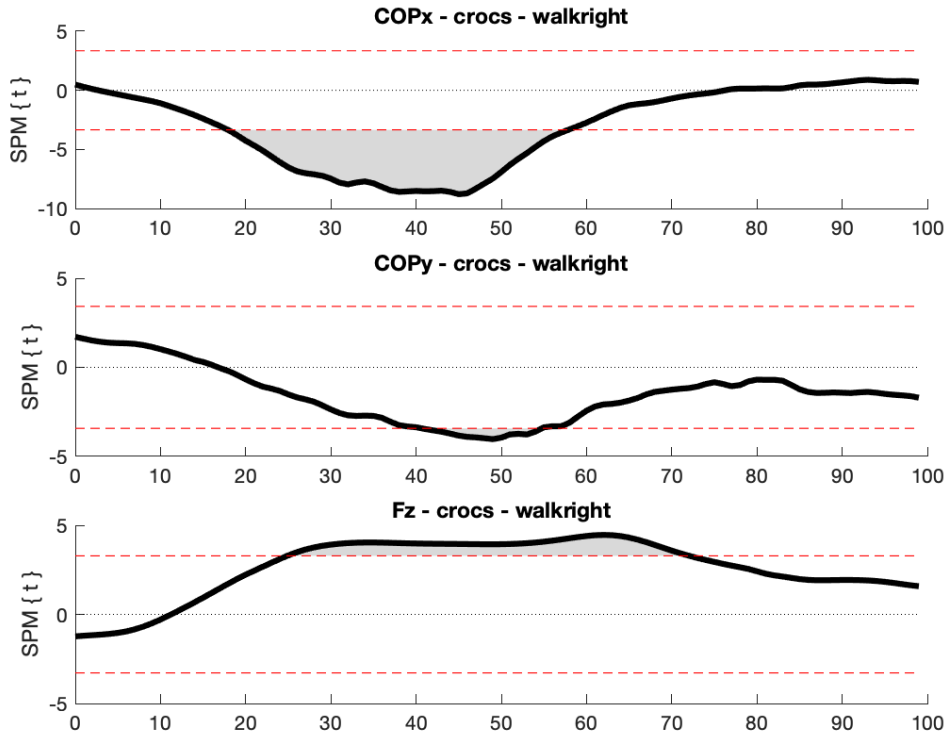

Figure 15. Statistical Parametric Mapping of COPx, COPy, and Fz in Crocs footwear during Walk right task.

4.3 Flat Shoes

4.3.1 Jump task. Table 7 presents the RMSD values of Flatshoe during the jump task. For the X-axis, an average of 40.09 ± 25.89 mm, while the values covered a range of 20.54 mm -117.60 mm ($p = 0.162$). Along the Y-axis, the values of RMSD fluctuated between 20.81 mm and 66.64 mm with a mean of 39.25 ± 12.00 mm ($p = 0.819$). Furthermore, the vertical force RMSD values spanned from 10.78 %BW to 187.90 %BW resulting in an average of 39.69 ± 43.61 %BW throughout all subjects ($p = 0.695$).

The SPM analysis for the Flatshoe condition during the jump task revealed no significant differences in COPx, COPy, or Fz between the Pedar insole and the force plate (Figure 16).

Table 8

Flat shoe RMSDx, RMSDy, and RMSDFz across jump tasks

Subject ID	RMSDx (mm)	RMSDy (mm)	RMSDFz (%BW)
1	54.28	30.89	59.00
2	35.04	33.13	25.67
3	24.27	33.05	18.52
4	23.11	39.93	46.37
5	47.40	50.76	12.53
6	20.54	39.60	32.55
7	45.37	56.21	36.63
8	25.26	20.81	17.53
9	23.04	35.47	33.26
10	117.60	66.64	53.78
11	36.68	41.98	24.89
12	71.64	46.78	187.90
13	27.44	28.92	12.02
14	25.64	38.53	23.85
15	23.99	26.12	10.78
Mean (SD)	40.09 (± 25.89)	39.25 (± 12.00)	39.69 (± 43.61)

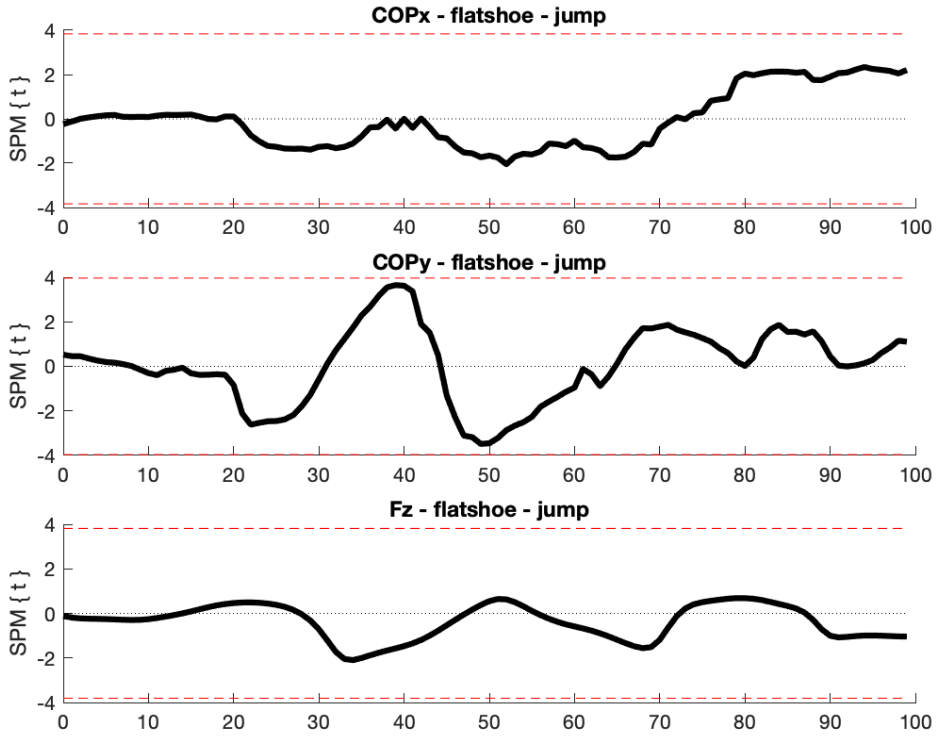

Figure 16. Statistical Parametric Mapping of COPx, COPy, and Fz in Flatshoe footwear during Jump task.

4.3.2 Single leg jump left task. During this task, Flatshoe exhibited mean RMSD values of 68.25 ± 24.80 mm (p = 0.043), 91.85 ± 39.71 mm (p = 0.017), and 67.28 ± 44.43 %BW (p = 0.206) among all subjects and corresponding ranges of 19.60 mm- 102.97 mm, 35.44 mm- 178.23 mm, and 12.80 %BW – 190.28 %BW, along X-axis, Y-axis and Fz respectively (Table 8).

The SPM analysis for the Flatshoe condition during the Single Leg Jump left task revealed large significant differences in COPx (~19–67% and ~93–100%) and in COPy at the beginning (~0–2%) and midpart of the cycle (~25–64%). Additionally, significant differences in Fz were also observed during the beginning of the cycle (~20–70%) (Figure 17).

Table 9

Flat shoe RMSDx, RMSDy, and RMSDFz across Single Leg Jump left tasks

Subject ID	RMSDx (mm)	RMSDy (mm)	RMSDFz (%BW)
1	81.43	178.23	190.28

Table 8 (cont'd)

Subject ID	RMSDx (mm)	RMSDy (mm)	RMSDFz (%BW)
2	72.73	124.97	90.23
3	69.72	74.72	43.30
4	43.12	103.02	19.12
5	93.21	150.73	35.98
6	64.42	118.79	95.59
7	74.54	99.83	88.93
8	102.97	51.41	12.80
9	27.15	86.85	65.84
10	19.60	56.35	90.08
11	62.53	99.44	19.11
12	81.57	35.44	77.96
13	52.83	85.16	60.51
14	105.38	48.51	40.39
15	72.49	64.37	79.13
Mean (SD)	68.25 (± 24.80)	91.85 (± 39.71)	67.28 (± 44.43)

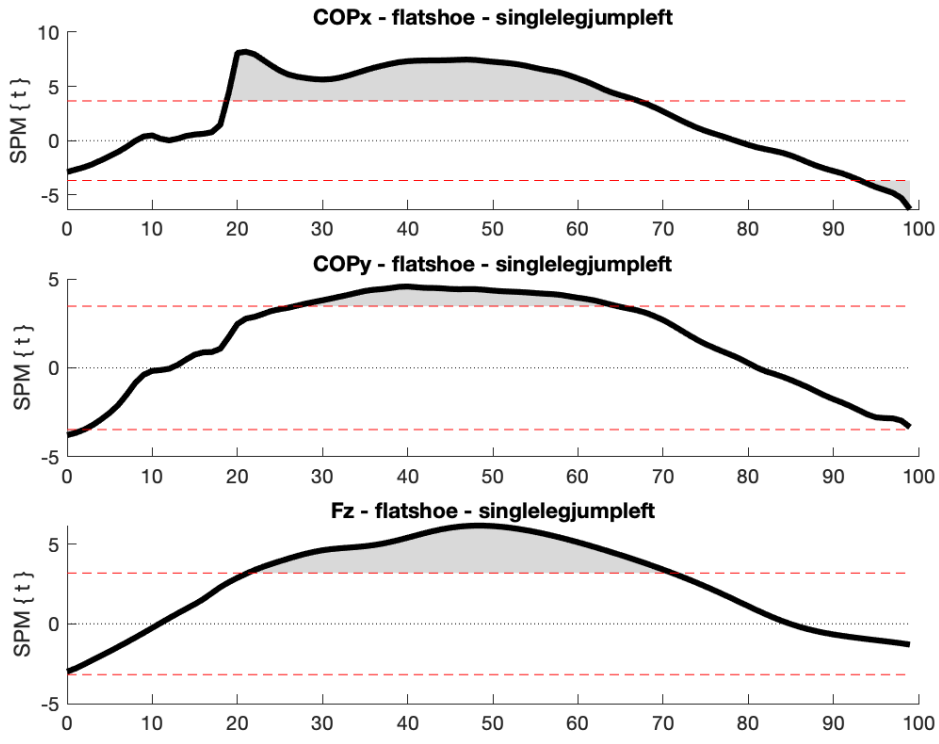

Figure 17. Statistical Parametric Mapping of COPx, COPy, and Fz in Flatshoe footwear during Single Leg Jump Left task.

4.3.3 Single leg jump right task. The average RMSD values computed for Flatshoe during this task ranged between 54.63 mm and 124.01 mm along the X-axis ($p = 0.758$), 28.08 mm and 196.28 mm along the Y-axis ($p = 0.247$), and 14.22 %BW – 156.99 %BW ($p = 0.743$) in the vertical force component across all participants, with average means of 87.95 ± 21.06 mm, 108.57 ± 47.32 mm, and 68.12 ± 42.07 %BW, respectively. (Table 9).

The SPM analysis for the Flatshoe condition during the Single Leg Jump right task revealed minimal significant differences in COPx at the beginning of the cycle (~0–1%), and large significant differences around the mid (~21–69%) and late (~95–100%) regions. COPy showed significant differences at the beginning (~0–8%), mid (~35–72%), and end (~98–100%) of the cycle. Significant differences in Fz were noted during the mid part of the cycle (~20–67%) (Figure 18).

Table 10

Flat shoe RMSDx, RMSDy, and RMSDFz across Single Leg Jump right tasks

Subject ID	RMSDx (mm)	RMSDy (mm)	RMSDFz (%BW)
1	109.61	156.60	156.99
2	78.16	110.12	69.55
3	63.67	119.44	24.10
4	109.90	167.74	135.29
5	84.39	85.62	24.71
6	124.01	196.28	106.80
7	81.10	115.74	55.62
8	100.79	28.43	14.22
9	94.92	111.16	70.98
10	55.98	102.90	62.82
11	54.63	112.02	17.59
12	82.71	28.08	73.74
13	87.57	135.69	83.66
14	114.80	49.75	39.71
15	76.97	108.93	85.97
Mean	87.95	108.57	68.12
(SD)	(± 21.06)	(± 47.32)	(± 42.07)

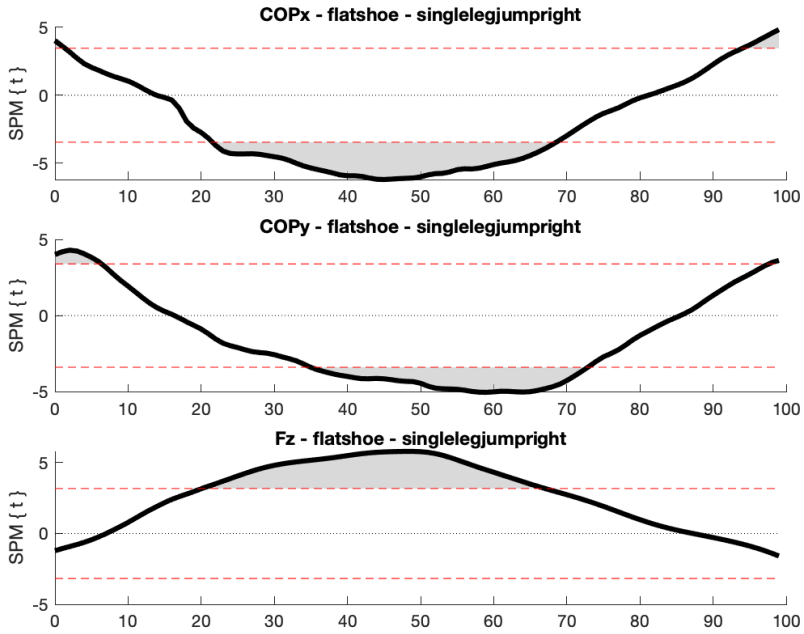

Figure 18. Statistical Parametric Mapping of COPx, COPy, and Fz in Flatshoe footwear during Single Leg Jump Right task.

4.3.4 Walk left task. As presented in Table 10, Flatshoe yielded a mean RMSDx value of 75.42 ± 19.77 mm (range: 49.64 mm and 119.07 mm; p = 0.084), and a mean RMSDy value of 83.49 ± 39.69 mm (range: 24.37 mm and 120.84 mm; p = 0.127), and a mean RMSDFz value of 50.95 ± 21.38 %BW (range: 22.52 %BW – 91.36 %BW; p = 0.221) among all subjects during this task.

The SPM analysis for the Flatshoe condition during thids task revealed significant differences in COPx around the region (~20–65%) of the cycle. As for COPy, minimal significant differences were observed around midstance of the cycle(~30–70%). On the other hand, large significant differences in Fz were observed during the midstanceof the cycle (~16–81%) (Figure 19).

Table 11

Flat shoe RMSDx, RMSDy, and RMSDFz across Walk left tasks

Subject ID	RMSDx (mm)	RMSDy (mm)	RMSDFz (%BW)
1	68.36	161.52	91.36
2	59.53	95.77	87.20

Table 10 (cont'd)

Subject ID	RMSDx (mm)	RMSDy (mm)	RMSDFz (%BW)
3	59.21	120.84	34.38
4	51.47	80.23	38.07
5	74.72	94.32	26.81
6	58.14	93.86	79.53
7	87.20	24.37	54.76
8	71.52	105.94	53.49
9	119.07	28.40	40.59
10	85.56	106.24	38.88
11	80.58	96.77	40.83
12	49.64	105.31	68.65
13	98.39	29.74	41.79
14	68.08	81.08	45.34
15	99.89	27.92	22.52
Mean (SD)	75.42 (± 19.77)	83.49 (± 39.69)	50.95 (± 21.38)

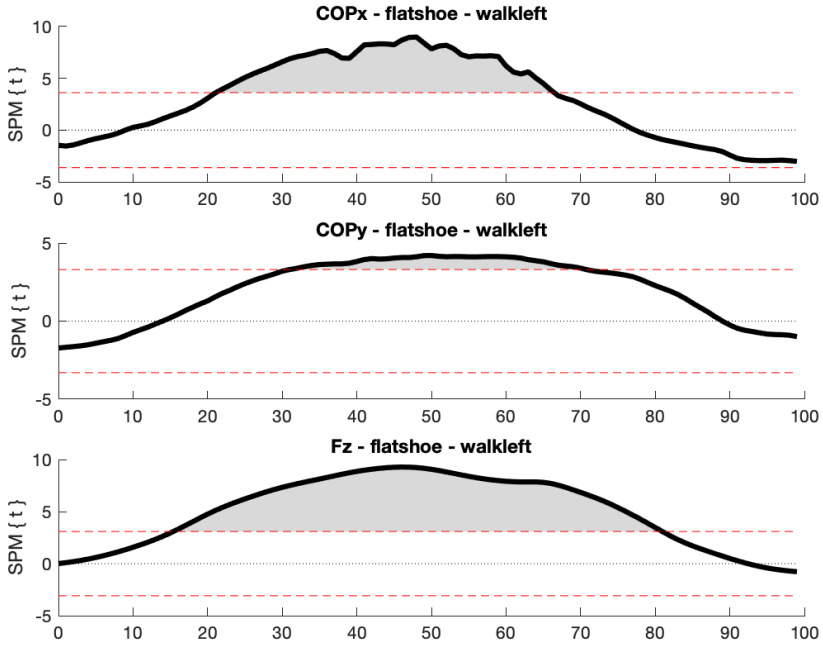

Figure 19. Statistical Parametric Mapping of COPx, COPy, and Fz in Flatshoe footwear during Walk Left task.

4.3.5 Walk right task. In this task, among all subjects, an average RMSDx of 71.09 ± 17.62 mm, ranging between 45.98 mm and 102.07 mm was found (p = 0.302). The mean RMSD value along the Y-axis was 81.93 ± 34.92 mm, ranging between (24.60 mm and 115.86 mm; p = 0.766). Meanwhile The mean RMSDFz value was found to be 46.96 ± 18.50 %BW (p = 0.280) extending from 28.55 %BW to 93.22 %BW (Table 11).

The SPM analysis for the Flatshoe condition during the Walk Right task revealed large significant differences around the regions (~15–72%) in the COPx between the Pedar insole and the force plate. In a contrasting manner, COPy showed minimal significant differences during the cycle (~52–68%). Conversely, large significant differences in Fz were observed between the Pedar insole and the force plate in the range (~12–80%) (Figure 20).

Table 12

Flat shoe RMSDx, RMSDy, and RMSDFz across Walk right tasks

Subject ID	RMSDx (mm)	RMSDy (mm)	RMSDFz (%BW)
1	60.66	109.11	44.18
2	77.74	115.10	67.03

Table 11 (cont'd)

Subject ID	RMSDx (mm)	RMSDy (mm)	RMSDFz (%BW)
3	48.25	109.49	29.96
4	51.14	94.93	32.83
5	91.35	95.70	28.55
6	58.28	89.89	93.22
7	80.49	26.67	54.88
8	69.93	91.93	44.68
9	96.12	30.57	68.30
10	75.06	115.86	33.85
11	76.30	106.11	29.72
12	45.98	91.98	47.56
13	78.81	24.60	57.63
14	54.12	98.50	41.79
15	102.07	28.48	30.18
Mean (SD)	71.09 (± 17.62)	81.93 (± 34.92)	46.96 (± 18.50)

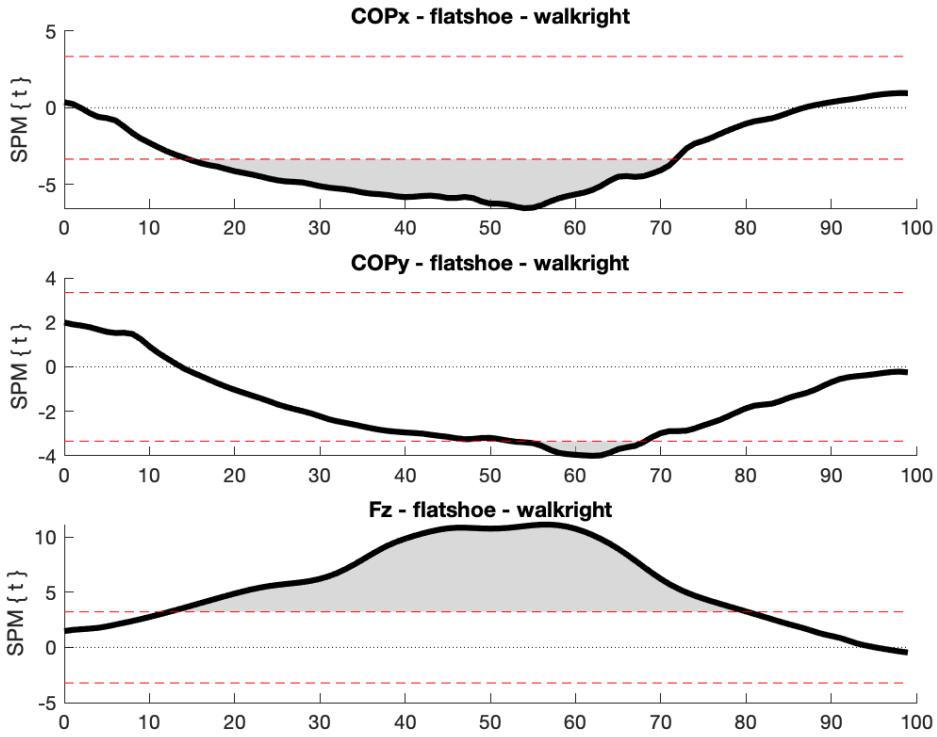

Figure 20 Statistical Parametric Mapping of COPx, COPy, and Fz in Flatshoe footwear during Walk Right task

4.4 Running Shoe

4.4.1 Jump task. The RMSDx values for running shoe during this task for all participants ranged between 20.82 mm and 86.04 mm with an average of 36.86 ± 18.37 mm ($p = 0.162$). However, The RMSD values of this footwear along the Y-axis were considerably higher with a mean of 43.17 ± 14.17 mm ($p = 0.819$) and values varying between (27.42 mm and 85.53 mm). The vertical force component displayed a mean RMSDFz value of 53.38 ± 31.65 %BW with values ranging between (14.66 %BW – 122.65 %BW) ($p = 0.695$) (Table 12).

The SPM analysis for the running shoe condition during the jump task revealed no significant differences in the COPx between the Pedar insole and the force plate. In the COPy, significant differences were found in only 2% of the cycle (~39-40%) and (~49-50%) between the Pedar insole and the force plate. Likewise, minimal significant differences were observed in Fz between the Pedar insole and the force plate (~33-36%) (Figure 21).

Table 13

Running shoe RMSDx, RMSDy, and RMSDFz across Jump tasks

Subject ID	RMSDx (mm)	RMSDy (mm)	RMSDFz (%BW)
1	61.74	46.64	67.67
2	30.57	46.53	69.43
3	22.52	39.14	43.60
4	33.21	31.33	20.20
5	39.31	47.43	15.43
6	23.36	33.38	107.75
7	38.89	35.04	38.60
8	30.86	43.92	53.65
9	86.04	85.53	122.65
10	21.44	46.21	55.20
11	54.84	52.67	73.04
12	25.25	35.63	14.66
13	41.95	48.51	45.27
14	22.04	28.17	21.83
15	20.82	27.42	51.70
Mean (SD)	36.86 (± 18.37)	43.17 (± 14.17)	53.38 (± 31.65)

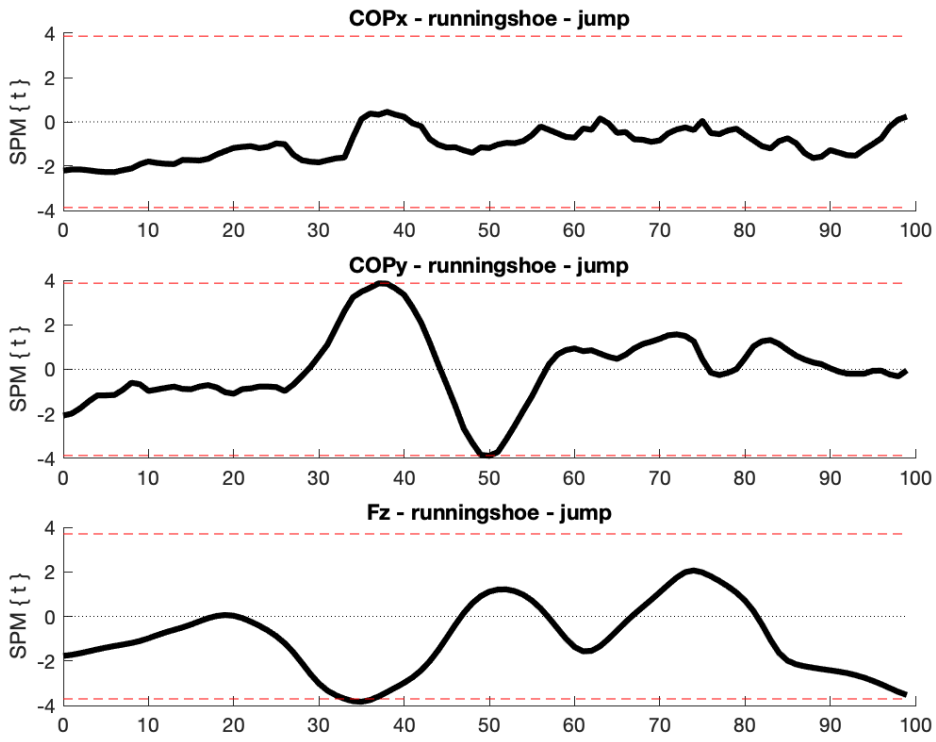

Figure 21. Statistical Parametric Mapping of COPx, COPy, and Fz in Running shoe footwear during Jumping task.

4.4.2 Single leg jump left task. The error metric calculated along the X-axis in this task ranged between 30.19 mm and 110.24 mm with a mean of 72.07 ± 21.09 mm (p = 0.043). Subsequently, an average RMSD value of 92.56 ± 36.18 mm was computed along the Y-axis (p = 0.017) with values ranging between 44.36 mm and 147.16 mm. Meanwhile, the mean RMSDFz value for this task was found to be 82.95 ± 47.05 (p = 0.206) %BW with values varying between 17.38 %BW – 174.97 %BW across all subjects (Table 13).

The SPM analysis for the running shoe condition during the Single Leg Jump left task revealed minimal significant differences in the COPx around multiple regions (~16-23%), (~29-34%), (~55-50%), and (~95-100%) between the Pedar insole and the force plate. Significant differences in the COPy were observed in 36% of the cycle (~15-41%) and (~90-100%) between the Pedar insole and the force plate. Additionally,

large significant differences in Fz were noted between the Pedar insole and the force plate (~20-68%) (Figure 22).

Table 14

Running shoe RMSDx, RMSDy, and RMSDFz across Single Leg Jump left tasks

Subject ID	RMSDx	RMSDy	RMSDFz
1	57.36	110.48	174.97
2	74.21	118.50	84.12
3	48.39	110.37	17.38
4	56.11	84.05	45.00
5	72.97	117.00	72.50
6	92.65	46.38	63.95
7	64.23	108.43	45.01
8	105.86	44.36	88.97
9	76.52	138.23	133.23
10	30.19	65.90	114.36
11	80.21	147.16	74.88
12	80.89	38.25	76.53
13	58.31	98.45	30.79
14	110.24	44.50	52.58
15	72.90	116.32	169.98
Mean (SD)	72.07 (± 21.09)	92.56 (± 36.18)	82.95 (± 47.05)

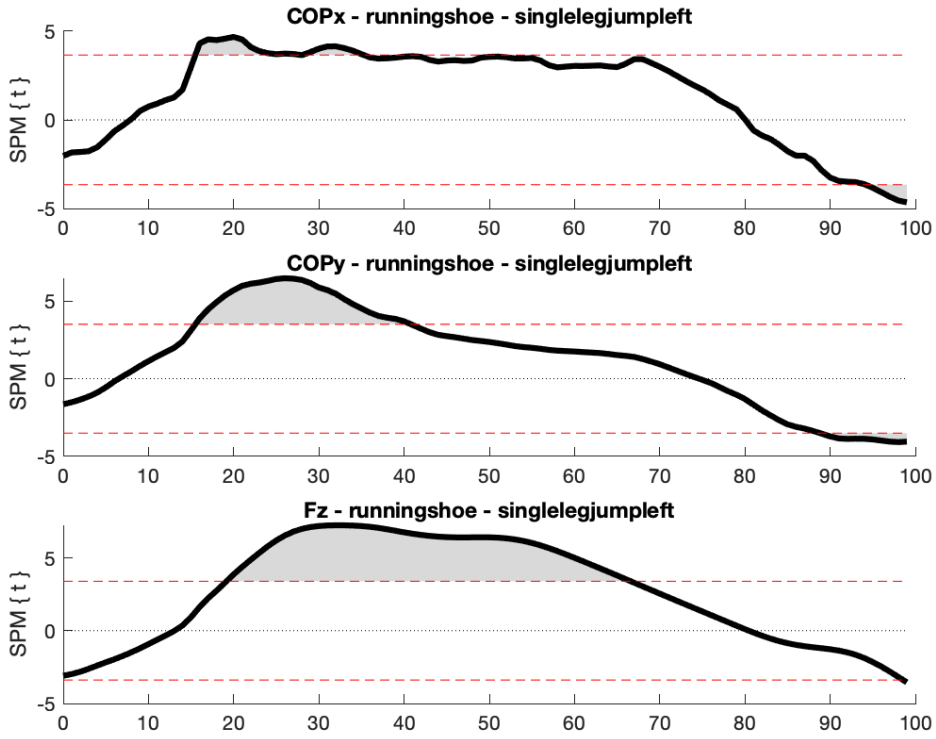

Figure 22. Statistical Parametric Mapping of COPx, COPy, and Fz in Running shoe footwear during Single Leg Jump left task

4.4.3 Single leg jump right task. In the Single Leg Jump Right task and among all subjects, the mean RMSDx value for the running shoe was 87.63 ± 27.06 mm (p = 0.758) covering a range from 55.62 mm to 158.58 mm. The RMSDy values were noticeably higher with a mean of 119.58 ± 44.44 (p = 0.247) mm and values varying within the range of 41.68 mm and 166.65 mm. As for the Fz, lower RMSD values were demonstrated with an average of 75.66 ± 56.86 %BW (p = 0.743) and values ranging between 10.80 mm and 180.90 mm (Table 14).

The SPM analysis for the running shoe condition during this task revealed minimal significant differences around (~50-54%) in the COPx between the Pedar insole and the force plate. No significant differences were found in the COPy between the Pedar insole and the force plate. Significant differences in Fz were observed

between the Pedar insole and the force plate around (~25-72%) of the cycle (Figure 23).

Table 15

Running shoe RMSDx, RMSDy, and RMSDFz across Single Leg Jump right tasks

Subject ID	RMSDx (mm)	RMSDy (mm)	RMSDFz (%BW)
1	103.89	166.65	170.15
2	126.18	148.89	160.75
3	98.39	164.50	180.90
4	61.83	119.27	22.81
5	64.65	111.45	22.77
6	80.61	119.26	42.85
7	77.66	159.92	74.48
8	90.97	42.66	42.93
9	77.71	131.06	52.43
10	158.58	44.84	70.79
11	74.45	139.63	24.70
12	61.68	139.15	95.94
13	91.22	164.37	116.18
14	91.03	41.68	46.35
15	55.62	100.40	10.80
Mean (SD)	87.63 (± 27.06)	119.58 (± 44.44)	75.66 (± 56.86)

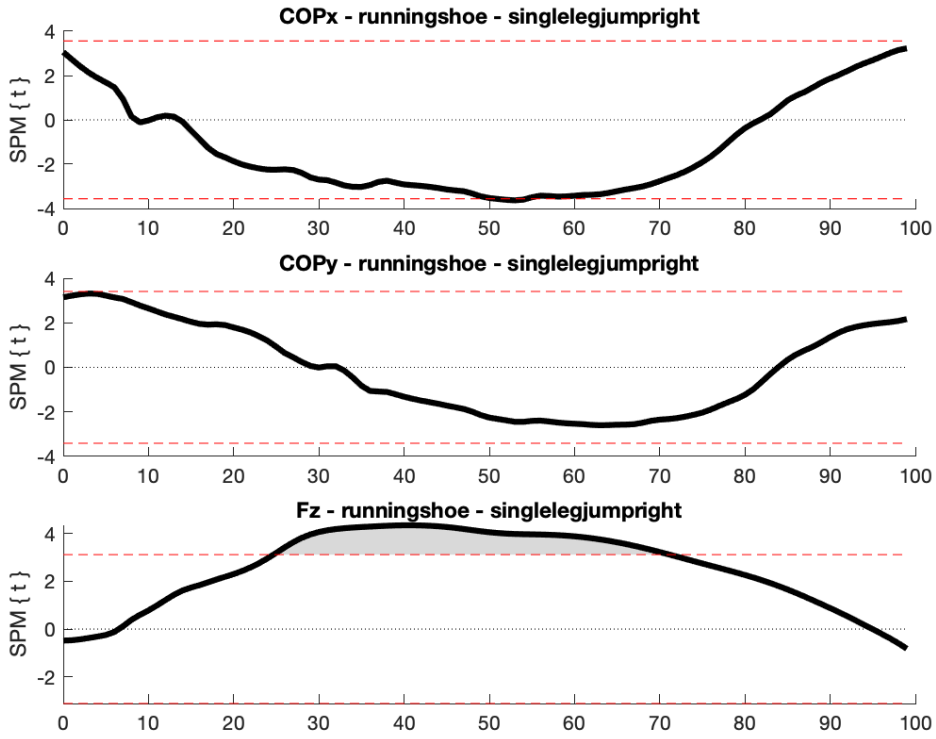

Figure 23. Statistical Parametric Mapping of COPx, COPy, and Fz in Running shoe footwear during Single Leg Jump right task.

4.4.4 Walk left task. Table 15 reports that the runningshoe during this task demonstrated close RMSDx, and RMSDy values with a relatively smaller RMSDFz values across all subjects. The means computed were 84.39 ± 18.75 mm (p = 0.084), 91.77 ± 42.84 mm (p = 0127), 62.59 ± 35.26 %BW (p = 0.221) with ranges spanning from (62.14 mm- 122.44 mm), (31. 07 mm and 159.78 mm), (26.73 %BW, 130.94 %BW), respectively.

The SPM analysis for the running shoe condition during the Walk Left task revealed no significant differences, although it approached significant points around (~50-60%) in the COPx between the Pedar insole and the force plate. Minimal significant differences were found in the COPy between the Pedar insole and the force plate in the ranges (~41-50%) and (~53-56%). Large significant differences in Fz were observed during large parts of the cycle (~15-79%) (Figure 24).

Table 16

Running shoe RMSDx, RMSDy, and RMSDFz across Walk left tasks

Subject ID	RMSDx (mm)	RMSDy (mm)	RMSDFz (%BW)
1	115.88	159.78	127.89
2	62.42	94.08	75.59
3	67.62	120.16	37.25
4	62.93	70.01	56.73
5	68.02	102.15	26.93
6	89.73	100.62	74.19
7	96.34	37.72	45.92
8	88.95	125.97	114.73
9	122.44	29.54	57.87
10	86.87	134.38	38.19
11	75.58	109.53	46.66
12	79.29	140.03	130.94
13	96.67	32.82	41.55
14	62.14	88.68	37.63
15	90.96	31.07	26.73
Mean (SD)	84.39 (± 18.75)	91.77 (± 42.84)	62.59 (± 35.26)

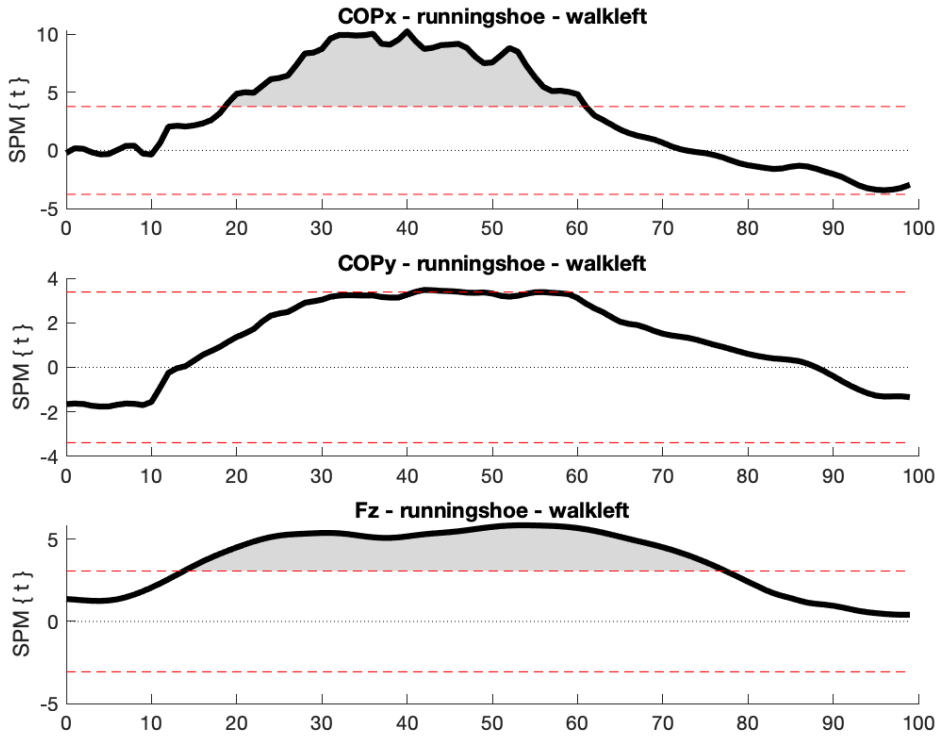

Figure 24 Statistical Parametric Mapping of COPx, COPy, and Fz in Running shoe footwear during Walk left task

4.4.5 Walk right task. According to Table 16, The mean RMSDx value computed for this task was 81.26 ± 29.40 mm (p = 0.302) with values extending from 42.95 mm and 134.83 mm. Similarly, the mean RMSDy value was 83.97 ± 36.86 mm (p = 0.766) with values extending from 28.44 mm and 149.01 mm. Remarkably, an average RMSDFz value of 52.62 ± 33.35 %BW was found with values fluctuating between 22.34 %BW – 144.86 %BW in all subjects (p = 0.280).

The SPM analysis for the running shoe condition during the Walk Right task revealed large significant differences in COPx around the regions (~23-57%) and (~63-65%) between the Pedar insole and the force plate. No significant differences were observed in the COPy between the Pedar insole and the force plate. Large significant deviations in Fz were found during the cycle (~17-72%) (Figure 25).

Table 17

Running shoe RMSDx, RMSDy, and RMSDFz across Walk right tasks

Subject ID	RMSDx (mm)	RMSDy (mm)	RMSDFz (%BW)
1	134.83	149.01	144.86
2	58.15	93.92	63.69
3	52.01	104.11	28.26
4	42.95	88.81	33.72
5	70.50	87.80	37.58
6	93.27	93.16	109.57
7	132.68	32.54	57.34
8	68.48	91.88	35.02
9	125.67	35.34	55.31
10	69.05	111.35	30.84
11	85.13	128.81	26.74
12	58.71	97.34	46.17
13	80.74	28.44	43.75
14	56.94	88.32	54.18
15	89.84	28.78	22.34
Mean (SD)	81.26 (± 29.40)	83.97 (± 36.86)	52.62 (± 33.35)

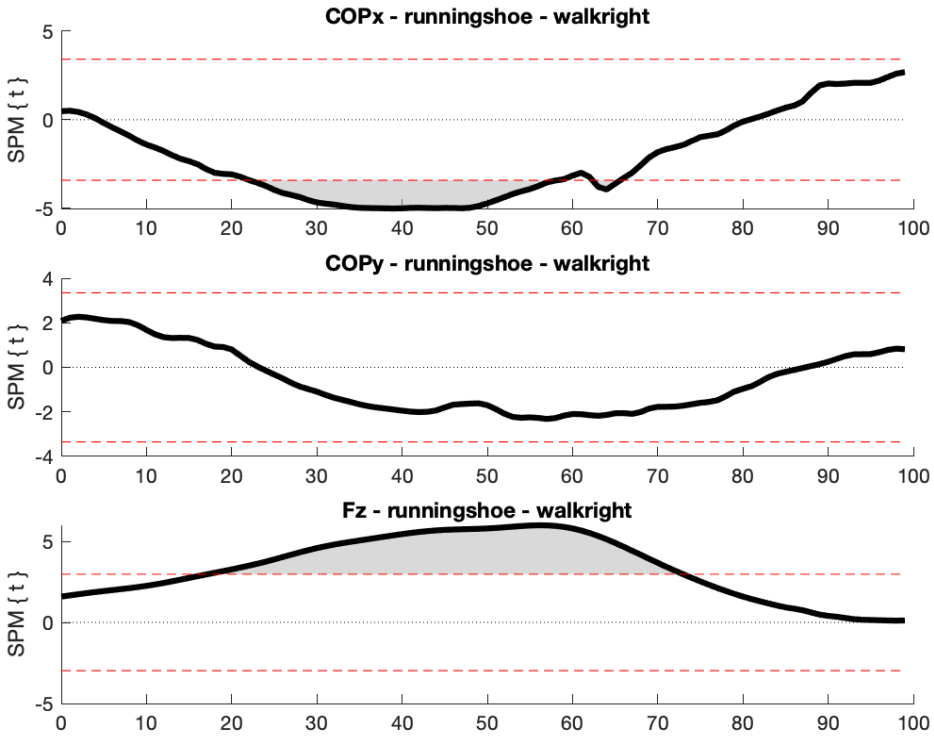

Figure 25. Statistical Parametric Mapping of COPx, COPy, and Fz in Running shoe footwear during Walk right task.

Chapter 5

Discussion

5.1 Interpretation of Main Findings

The present study offers a comprehensive assessment of the impact of different footwear on the performance of pressure-measuring insoles (Pedar), against the gold standard (force plate). Three primary error metrics were analyzed: RMSDx and RMSDy, corresponding to the COP error along the ML and AP axes, and RMSDFz, corresponding to the reaction force error along the vertical axis. SPM revealed significant differences among the footwear conditions, with the flat shoe condition showing a pronounced deviation. This divergence is likely attributed to the absence of midsole cushioning, which may allow more direct pressure transmission and affect insole accuracy.

For COPx, the flat shoe yielded the lowest mean error (68.58 ± 7.36 mm), followed by running shoes (72.65 ± 12.88 mm) and Crocs (75.02 ± 18.31 mm). While conventional statistics previously showed no significant effect ($p = 0.247$), the SPM analysis highlighted regions of the stance phase where the flat shoe condition significantly differed, underscoring its unique impact on COPx measurements.

Along the y-axis (COPy), the highest error was observed in Crocs (89.14 ± 27.34 mm), followed by running shoes (85.96 ± 19.52 mm), with the flat shoe again producing the lowest mean error (81.44 ± 21.48 mm). Furthermore, SPM detected significant differences in specific temporal regions, suggesting that footwear structure particularly the lack of cushioning in flat shoes can subtly influence anteroposterior CoP measurements.

For vertical force (Fz), Crocs yielded the highest RMSD error (68.85 ± 38.10 %BW), followed by running shoes (63.53 ± 27.23 %BW), and flat shoes (54.26 ± 24.68 %BW). SPM confirmed significant deviations in Fz as well, particularly in the

flat shoe condition, reinforcing the hypothesis that midsole design modulates the accuracy of vertical force estimation by pressure insoles.

In summary, SPM analysis revealed that footwear type significantly influences pressure insole measurements. The flat shoe condition, characterized by the absence of cushioning, exhibited statistically significant deviations most notably in COPx and Fz emphasizing its role in direct pressure transmission and measurement fidelity during dynamic tasks.

5.2 Biomechanical Implications

In the study of biomechanics and human motion, shoes impact plantar pressure transmission across the insole to the ground, subsequently impacting the accuracy of pressure measurement.

The deviation noted along the ML axis, from the RMSDx findings illustrates that constructed shoes generate lower COP excursions, due to the absence of midsole cushioning and firmer design, hence a better ability to capture pressure data. Such findings support the previously reported findings that stated that footwear compliance is important for pressure measuring insoles accuracy.

Furthermore, the lowest RMSDy value observed was also from flatshoe, indicating that the subtle foot motion is clearly captured and not masked by the shoe cushioning.

Nevertheless, although footwear characteristics may impact the real time data transmission as observed in this study, it is also wise to take into consideration the insole system's limitations. Although the pressure measuring insoles were tested in many contexts and validated in such contexts. They may be susceptible to motion artifacts, specifically when exposed to unbalanced distribution of force.

Along the vertical axis, the RMSD values reflected the interplay between footwear design and sensor performance. The flat shoe condition exhibited the lowest RMSD, suggesting enhanced pressure transmission due to the absence of midsole

cushioning. These variations may be attributed to the insole's sensitivity to high-magnitude or rapidly applied forces.

In general, while the footwear design undeniably has an impact on the pressure measuring insoles, devices like Pedar are sensitive to contextual challenges (e.g. jumping tasks). In the present study, flatshoe appears to be a favorable option to combine with pressure measuring insoles, due to their simple design and hence allowing the insoles to capture clean data.

5.3 Sensor Performance Considerations

In the context of assessing the effect of different footwear on the accuracy of pressure measuring insoles, a study done by our research team (Chebel et. al, 2023) offered valuable insights. The research tested the impact of 4 conditions, barefoot, socks, flatshoe, and sneakers on pressure measuring insoles in static tasks. The socks conditions yielded the lowest RMSD values across COPx, COPy, and Fz. Indicating that a minimal shoe structure and midsole can reduce the motion artifacts and help provide a neater data in ideal conditions.

Direct contact between sensors and floor allows for an effective interaction between the system and the foot and reduces the likelihood of motion artifacts occurrence and footwear cushioning that alters the sensor readings. However, due to several methodological and practical considerations, the socks condition was excluded from this study. Dynamic tasks, such as jumping or walking without shoe support can exert high pressure on the insoles' sensor matrix, additionally the participants will have to adapt to an unnatural way of gait while performing these tasks in order to protect their feet or compensate for the lack of support provided usually by the footwear. Moreover, the use of socks in dynamic activities can shorten the lifespan of the insoles and negatively impact their long-term usability and hence contribute to their damage.

Altogether, while pressure insoles offer portable gait analysis solutions, their outcomes must be combined with footwear considerations to ensure accurate and highly reliable results.

5.4 Clinical and Research Applications

Sports biomechanics, clinical assessment, and rehabilitation using pressure insoles can benefit from the outcomes. The trends noted in this study illustrate that the footwear choice has the ability to impact the accuracy of pressure measurement.

Flatshoes provided the most stable COP results along X and Y-axis and hence seem like a favorable choice for standardized assessments.

Therefore, for research and clinical purposes, standardizing footwear during pressure measuring protocols seems to be critical. Such considerations can reduce measurement artifacts and ensure high-fidelity acquisition of biomechanical data.

Chapter 6

Conclusion and Future Directions

6.1 Conclusion

The impact of various footwear on pressure measuring insoles' accuracy during dynamic tasks was studied and compared by computing the RMSD of the Pedar-measured COPx, COPy, and Fz (RMSDx, RMSDy, and RMSDFz) in reference to the gold standard (force plate). The results revealed that footwear type influences the accuracy of the tested parameters, as confirmed by SPM analysis. Nevertheless, a moderate influence of footwear on the variability of measurements was noted. A summary of the drawn conclusions can be broken down as follow:

- In the X-axis, the RMSD values were the most consistent in the Flatshoe footwear condition.
- Along the Y-axis, Flatshoe footwear again provided the most consistent COP tracking, likely due to their firm design.
- As for the vertical component of force (Fz), Flatshoe yielded the lowest error, indicating that due to its design and absence of excessive cushioning, it allows for more direct and consistent pressure transmission to the insole sensors.

To sum up, pressure measuring insoles, such as Pedar can assess everyday dynamic tasks and provide valuable outcomes. However, careful considerations of footwear in both clinical and research settings to maximize the information obtained from this system.

6.2 Future Directions

According to the current outcomes, it is advised to conduct further studies that evaluates a larger number of populations including foot ulcer subjects, elderly individuals, and those with neurological or musculoskeletal impairment. Such groups

are likely more sensitive to footwear effects and provide a deeper insight into shoe structure and its interaction with pressure measuring insoles.

More dynamic tasks should be included in subsequent research such as stairs climbing, running, and combined running and jumping where higher magnitude of force is exerted on the pressure insoles and deviations induced by footwear can be observed.

Additionally, footwear properties such as heel to toe drop, outsole geometry, and excessive midsole cushioning must be taken into consideration when evaluating the impact of footwear on pressure measuring insoles accuracy. Such parameters may perhaps contribute to the construction of predictive calibration models by utilizing machine learning tools and subsequently offering adaptive insoles technology that can enhance measurements based on shoe characteristics.

Overall, the present study displays the important but often not considered impact of footwear on pressure measuring insoles performance in capturing dynamic tasks data. Future research aimed at larger population, various tasks, and advanced analysis is necessary to enhance the use of wearable pressure measuring insoles in clinical and research settings.

REFERENCES

Agresta, C., Giacomazzi, C., Harrast, M., & Zendler, J. (2022). Running Injury Paradigms and Their Influence on Footwear design features and runner Assessment Methods: A Focused Review to Advance Evidence-Based Practice for Running Medicine Clinicians. Frontiers in Sports and Active Living, 4. https://doi.org/10.3389/fspor.2022.815675

Bloks, B. E., Wilders, L. M., Louwerens, J. W. K., Geurts, A. C., Nonnekes, J., & Keijsers, N. L. (2023). Quantitative assessment of plantar pressure patterns in relation to foot deformities in people with hereditary motor and sensory neuropathies. *Journal of NeuroEngineering and Rehabilitation*, *20*(1), 65. https://doi.org/10.1186/s12984-023-01172-1

Castro-Martins, P., Marques, A., Coelho, L., Vaz, M., & Baptista, J. S. (2024). In-shoe plantar pressure measurement technologies for the diabetic foot: A systematic review. *Heliyon*, *10*(9). https://doi.org/10.1016/j.heliyon.2024.e29672

Chander, H., Arachchige, S. N. K. K., Turner, A. J., Burch, R. F., V., Knight, A. C., Wade, C., & Garner, J. C. (2021). Role of Occupational Footwear and Prolonged Walking on Lower Extremity Muscle Activation during Maximal Exertions and Postural Stability Tasks. Biomechanics, 1(2), 202–213. https://doi.org/10.3390/biomechanics1020017

Chebel, E., Jama, A. A. M., Kassem, O., & Tunc, B. (2023, November). Comparative Analysis of Footwear Effects on Wireless Pressure Insoles Performance. In *2023 Medical Technologies Congress (TIPTEKNO)* (pp. 1-4). IEEE.

Cho, Y. J., Lee, D., Shin, H. S., Hwang, Y. B., Lee, D. O., Kim, D., & Lee, D. Y. (2022). Change of In-Shoe plantar pressure according to types of shoes (Flat shoes, running shoes, and high heels). Clinics in Orthopedic Surgery, 14(2), 281. https://doi.org/10.4055/cios20260

Das, P. S., Skaf, D., Rose, L., Motaghedi, F., Carmichael, T. B., Rondeau-Gagné, S., & Ahamed, M. J. (2024). Gait pattern analysis: integration of a highly sensitive flexible pressure sensor on a wireless instrumented insole. *Sensors*, *24*(9), 2944. https://doi.org/10.3390/s24092944

Flores, N., Delattre, N., Berton, E., & Rao, G. (2018). Does an increase in energy return and/or longitudinal bending stiffness shoe features reduce the energetic cost of running? European Journal of Applied Physiology, 119(2), 429–439. https://doi.org/10.1007/s00421-018-4038-1

Forczek-Karkosz, W., Michnik, R., Nowakowska-Lipiec, K., Vargas-Macias, A., Baena-Chicón, I., Gómez-Lozano, S., & Gorwa, J. (2021). Biomechanical description of Zapateado technique in flamenco. *International Journal of Environmental Research and Public Health*, *18*(6), 2905. https://doi.org/10.3390/ijerph18062905

Gámez-Payá, J., Dueñas, L., Arnal-Gómez, A., & Benítez-Martínez, J. C. (2021). Foot and lower limb clinical and structural changes in overuse injured recreational runners using floating heel shoes: Preliminary results of a randomised control trial. *Sensors*, *21*(23), 7814. https://doi.org/10.3390/s21237814

Gregory, N. R. W., Axtell, N. R. S., Robertson, N. M. I., & Lunn, N. W. R. (2018). The effects of a carbon fiber shoe insole on athletic performance in collegiate

athletes. Journal of Sports Science, 6(4). https://doi.org/10.17265/2332-7839/2018.04.001

Hébert-Losier, K., Finlayson, S. J., Driller, M. W., Dubois, B., Esculier, J., & Beaven, C. M. (2020). Metabolic and performance responses of male runners wearing 3 types of footwear: Nike Vaporfly 4%. Journal of Sports Sciences, 1–9. https://doi.org/10.1016/j.jshs.2020.11.012

HIROSE, K., KAJIWARA, W., KONDO, A., NAKAMURA, Y., & TAKEDA, M. (2025). Sensor fusion for estimating ground reaction force using insole-type foot pressure and inertial sensors. *Mechanical Engineering Journal*, *12*(2), 24-00482. https://doi.org/10.1299/mej.24-00482

Honert, E. C., Mohr, M., Lam, W. K., & Nigg, S. (2020). Shoe feature recommendations for different running levels: A Delphi study. *PloS one*, *15*(7), e0236047. https://doi.org/10.1371/journal.pone.0236047

Hollander, K., Rahlf, A. L., Wilke, J., Edler, C., Steib, S., Junge, A., & Zech, A. (2021). Sex-specific differences in running injuries: a systematic review with meta-analysis and meta-regression. *Sports Medicine*, *51*, 1011-1039. https://doi.org/10.1007/s40279-020-01412-7

Horst, F., Lapuschkin, S., Samek, W., Müller, K. R., & Schöllhorn, W. I. (2019). Explaining the unique nature of individual gait patterns with deep learning. *Scientific reports*, *9*(1), 2391. https://doi.org/10.1038/s41598-019-38748-8

Jiang, Y., Wang, D., Ying, J., Chu, P., Qian, Y., & Chen, W. (2021). Design and preliminary validation of individual customized insole for adults with flexible

flatfeet based on the plantar pressure redistribution. *Sensors*, *21*(5), 1780. https://doi.org/10.3390/s21051780

Knopp, M., Muniz-Pardos, B., Wackerhage, H., Schönfelder, M., Guppy, F., Pitsiladis, Y., & Ruiz, D. (2023). Variability in running economy of Kenyan world-class and European amateur male runners with advanced footwear running technology: experimental and meta-analysis results. *Sports Medicine*, *53*(6), 1255-1271. https://doi.org/10.1007/s40279-023-01816-1

Lambrich, J., Hagen, M., Schwiertz, G., & Muehlbauer, T. (2023). Concurrent validity and test–retest reliability of pressure-detecting insoles for static and dynamic movements in healthy young adults. *Sensors*, *23*(10), 4913. https://doi.org/10.3390/s23104913

Li, J., Song, Y., Xuan, R., Sun, D., Teo, E. C., Bíró, I., & Gu, Y. (2022). Effect of long-distance running on inter-segment foot kinematics and ground reaction forces: A preliminary study. *Frontiers in Bioengineering and Biotechnology*, *10*, 833774. https://doi.org/10.3389/fbioe.2022.833774

Lieberman, D. E., Venkadesan, M., Werbel, W. A., Daoud, A. I., D'andrea, S., Davis, I. S., ... & Pitsiladis, Y. (2010). Foot strike patterns and collision forces in habitually barefoot versus shod runners. *Nature*, *463*(7280), 531-535. https://doi.org/10.1038/nature08723

Lin, S., Song, Y., Cen, X., Bálint, K., Fekete, G., & Sun, D. (2022). The implications of sports biomechanics studies on the research and development of running shoes: A systematic review. *Bioengineering*, *9*(10), 497. https://doi.org/10.3390/bioengineering9100497

Lindorfer, J., Kröll, J., & Schwameder, H. (2019). Comfort assessment of running footwear: Does assessment type affect inter-session reliability? *European journal of sport science*, *19*(2), 177-185. https://doi.org/10.1080/17461391.2018.1502358

Lippa, N., Bonacci, J., Collins, P. K., Rawlins, J. W., & Gould, T. E. (2019). Effect of mechanically aged minimalist and traditional footwear on female running biomechanics. *Proceedings of the Institution of Mechanical Engineers, Part P: Journal of Sports Engineering and Technology*, *233*(3), 375-388 https://doi.org/10.1177/1754337118824001

Malisoux, L., Delattre, N., Urhausen, A., & Theisen, D. (2020). Shoe cushioning influences the running injury risk according to body mass: a randomized controlled trial involving 848 recreational runners. *The American journal of sports medicine*, *48*(2), 473-480. https://doi.org/10.1177/0363546519892578

Menz, H. B., & Bonanno, D. R. (2021). Footwear comfort: a systematic search and narrative synthesis of the literature. *Journal of Foot and Ankle Research*, *14*, 1-11. https://doi.org/10.1186/s13047-021-00500-9

Miao, T., Wang, P., Zhang, N., & Li, Y. (2021). Footwear microclimate and its effects on the microbial community of the plantar skin. *Scientific Reports*, *11*(1), 20356. https://doi.org/10.1038/s41598-021-99865-x

Moisan, G., Descarreaux, M., & Cantin, V. (2020). The influence of footwear on walking biomechanics in individuals with chronic ankle instability. *PloS one*, *15*(9), e0239621. https://doi.org/10.1371/journal.pone.0239621

Morrison, S. C., Price, C., McClymont, J., & Nester, C. (2018). Big issues for small feet: developmental, biomechanical and clinical narratives on children's

footwear. *Journal of foot and ankle research*, *11*, 1-5. https://doi.org/10.1186/s13047-018-0281-2

Papagiannaki, M., Samoladas, E., Maropoulos, S., & Arabatzi, F. (2020). Running-related injury from an engineering, medical and sport science perspective. Frontiers in bioengineering and biotechnology, *8*, 533391. https://doi.org/10.3389/fbioe.2020.533391

Petersen, E., Zech, A., & Hamacher, D. (2020). Walking barefoot vs. with minimalist footwear–influence on gait in younger and older adults. *BMC geriatrics*, *20*, 1-6 https://doi.org/10.1186/s12877-020-1486-3

Polomé, E., Théveniau, N., Vigier, C., Dumas, R., & Robert, T. (2020). Influence of different footwear on mediolateral stability during gait at different speeds in healthy people. *Computer Methods in Biomechanics and Biomedical Engineering*, *23*(sup1), S226-S228. https://doi.org/10.1080/10255842.2020.1815318

Ramsey, C., Peterson, B., & Hebert-Losier, K. (2023). Measurement and reporting of footwear characteristics in running biomechanics: A systematic search and narrative synthesis of contemporary research methods. *Sports Biomechanics*, *22*(3), 351-387. https://doi.org/10.1080/14763141.2022.2125431

Reina-Bueno, M., Calvo-Lobo, C., López-López, D., Palomo-López, P., Becerro-de-Bengoa-Vallejo, R., Losa-Iglesias, M. E., ... & Navarro-Flores, E. (2021). Effect of foot orthoses and shoes in Parkinson's disease patients: a PRISMA systematic review. *Journal of Personalized Medicine*, *11*(11), 1136. https://doi.org/10.3390/jpm11111136

Salis, F., Bertuletti, S., Bonci, T., Caruso, M., Scott, K., Alcock, L., ... & Cereatti, A. (2023). A multi-sensor wearable system for the assessment of diseased gait in real-world conditions. *Frontiers in Bioengineering and Biotechnology*, *11*, 1143248. https://doi.org/10.3389/fbioe.2023.1143248

Sinclair, J. K., & Taylor, P. (2025). Exploration of running in minimal and conventional footwear on tibial stress fracture probability in habitual and non-habitual minimal users. *Baltic Journal of Health & Physical Activity*, *17*(1). https://www.doi.org/10.29359/BJHPA.17.1.5

Soltani, N., Jalalvand, A., & Jahani, M. R. (2021). Comparison of Plantar Force, Pressure and Impulse During Walking in Men and Women With Flat Feet. *Journal of Sport Biomechanics*, *7*(2), 94-107. https://doi.org/10.32598/biomechanics.7.1.2

Van Alsenoy, K., Ryu, J. H., & Girard, O. (2022). Acute intense fatigue does not modify the effect of EVA and TPU custom foot orthoses on running mechanics, running economy and perceived comfort. *European* Journal of Applied Physiology, *122*(5), 1179-1187. https://doi.org/10.1007/s00421-022-04903-9

Verheul, J., Nedergaard, N. J., Vanrenterghem, J., & Robinson, M. A. (2020). Measuring biomechanical loads in team sports–from lab to field. Science and Medicine in Football, 4(3), 246-252. https://doi.org/10.1080/24733938.2019.1709654

Zhang, M., Shi, H., Liu, H., & Zhou, X. (2021). Biomechanical analysis of running in shoes with different heel-to-toe drops. *Applied Sciences*, *11*(24), 12144. https://doi.org/10.3390/app112412144

Zwaferink, Jennefer BJ, et al. "Optimizing footwear for the diabetic foot: Data-driven custom-made footwear concepts and their effect on pressure relief to prevent diabetic foot ulceration." *PLoS One* 15.4 (2020): e0224010. https://doi.org/10.1371/journal.pone.0224010

Zwaferink, J. B., Nollet, F., & Bus, S. A. (2024). In-Shoe Pressure Measurements in Diabetic Footwear Practice: Success Rate and Facilitators of and Barriers to Implementation. *Sensors*, *24*(6), 1795. https://doi.org/10.3390/s24061795